Simulating decadal cross-shore dynamics at nourished coasts with Crocodile

Kettler, Tosca; de Schipper, Matthieu; Luijendijk, Arjen

DOI
10.1016/j.coastaleng.2024.104491

Publication date
2024

Document Version
Final published version

Published in
Coastal Engineering

Citation (APA)
Kettler, T., de Schipper, M., & Luijendijk, A. (2024). Simulating decadal cross-shore dynamics at nourished coasts with Crocodile. *Coastal Engineering*, *190*, Article 104491. https://doi.org/10.1016/j.coastaleng.2024.104491

Coastal Engineering 190 (2024) 104491

Contents lists available at ScienceDirect

Coastal Engineering

journal homepage: www.elsevier.com/locate/coastaleng

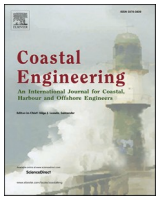

Simulating decadal cross-shore dynamics at nourished coasts with Crocodile

Tosca Kettler [a,*], Matthieu de Schipper [a], Arjen Luijendijk [a,b]

[a] TU Delft, the Netherlands
[b] Deltares, the Netherlands

ARTICLE INFO

Keywords:
Diffusion model
Nourishment strategies
Sand dispersion
Numerical modelling
Cross-shore profile

ABSTRACT

Projections of high rates of sea level rise have stimulated proposals for adaptation strategies with increasingly high nourishment volumes along sandy beaches. An underlying assumption is that coastal profiles respond rapidly to nourishments by redistributing sediments towards a (new) equilibrium shape. However, this perception may not be valid when high volumes of nourishment are applied, as the profile shape may then undergo significant deformation. Current state-of-the-art modelling techniques often concentrate on a single spatio-temporal scale, either lacking the necessary temporal horizon or failing to provide the required level of cross-shore detail. This article introduces Crocodile, a diffusion based cross-shore model designed to bridge the gap between short- and long-term nourishment modelling. The model simulates the effects of nourishment strategies on coastal volume, coastline position and beach width over a decadal timeframe. It incorporates different elements which compute cross-shore diffusion, sediment exchange with the dune and longshore sediment losses. To test the model performance, a series of idealized nourishment scenarios are examined, along with three case studies along the Dutch coast with different nourishment strategies over the past few decades. The modelled coastal volume, shoreline position and beach width strongly resemble the observations with only a 12% overestimation in profile volume and 13% underestimation in beach width. Averaged over selected periods of nourishment, trends and trend reversals between different strategies are well replicated with slight overestimation for coastal volume trends by 1.5 $m^3/m/yr$ (10%), while beach width trends are underestimated by 0.2 m/yr (15%). Given that the added nourishment volumes are typically in the order of 100 m^3/m, these model errors are considered sufficiently low to conclude that Crocodile effectively simulates variations in coastal volume, coastline position and beach width over a decadal timeframe in response to different nourishment strategies. Therefore, Crocodile can facilitate the evaluation of future nourishment strategies.

1. Introduction

At a time of accelerating sea level rise (IPCC AR6 Working Group I, 2021), growing coastal populations (IPCC AR6 Working Group II, 2022), and rising concerns about coastal squeeze (Doody, 2013), sustainable coastal management is one of the most important issues facing the world. One such solution is sand nourishment, which involves the placement of sand on the foreshore, beach, or dune to build up or maintain the coastal sediment budget as well as the position of the shoreline. Under the force of waves, winds and currents, the sand is dispersed in longshore and cross-shore directions (van Duin et al., 2004). Over the coming decades, the anticipated acceleration of sea level rise is likely to shorten the lifespan of individual nourishments (Haasnoot et al., 2020) prompting proposals for adaptation strategies that involve higher nourishment volumes. These adaptation strategies involve various design considerations, such as the amount of sand volume applied, the expected frequency of nourishment, and the location of the nourishment along the cross-shore profile. The rationale behind these design choices follows from the accessibility of materials and knowledge and the objectives of coastal management, which may involve addressing coastal erosion, preserving a particular beach width, or stabilizing the coastline (Brand et al., 2022; Cooke et al., 2012; Defeo et al., 2009; Hanson et al., 2002). These objectives can be guided or evaluated by coastal state indicators such as coastline position, beach width and profile volume change, as they are closely linked to issues of coastal safety (e.g., Van Koningsveld and Mulder, 2004), ecology (e.g.,Schooler

* Corresponding author.
E-mail address: T.T.Kettler@TUDelft.nl (T. Kettler).

https://doi.org/10.1016/j.coastaleng.2024.104491
Received 8 October 2023; Received in revised form 30 January 2024; Accepted 22 February 2024
Available online 6 March 2024

et al., 2019), and socioeconomics (e.g., Cabezas-Rabadán et al., 2019; McLachlan et al., 2013; Valdemoro and Jiménez, 2006). In the design phase of nourishment programs, it is therefore desirable to have prior knowledge of the corresponding response of these coastal state indicators to evaluate the effectiveness of nourishment programs. With this study, we aim to fulfil this need. We develop a tool to examine the decadal-scale response of coastal indicators to nourishment programs and test its performance at case study locations along the central Dutch coast.

1.1. Temporal evolution of nourishment across different timescales

An increasing number of nourishments has been executed and has been described in the scientific literature (De Schipper et al., 2014; Hamm et al., 2002; Luo et al., 2016; Stronkhorst et al., 2018; Valverde et al., 1999). However, quantifying the impacts of nourishment schemes is yet challenging because of the complexity and variability of the physical processes involved, acting within a broad spatiotemporal range. Consequently, most traditional methods that compute sediment transport and morphological behaviour in the coastal zone focus on a specific spatiotemporal scale and do not capture the broad temporal spectrum (~years-decades) required to offer a holistic view on the effects of design choices in nourishment schemes. To illustrate the nature of the uncertain relation between coastal state indicators and nourishment, we examine it from multiple time perspectives.

Short-term (days to years) and small-scale (0.1–1 km) processes can be exemplified by the immediate impacts of storms on a nourished coastal profile, as well as the evolution of bays and lagoons that may be present. Directly after the placement of a beach nourishment, the beach is widened, and the volume of the coastal profile is increased. This sand is rapidly redistributed from the beach to the nearshore when storm frequency is high. This can result in a notable decrease in beach width and shoreline retreat over a short period of time. Despite of this redistribution, the sand often remains in the active profile region over this timeframe. In the case of shoreface nourishments, these short-term effects are typically less visible.

On the medium-term (months to years), changes in the local sediment budget typically become visible in the behaviour of profile volume, beach width and coastline. This sediment budget includes sediment supply and losses via gradients in longshore transport by wind, waves, and tidal currents. A positive sediment budget is generally correlated to an increasing beach width and seaward shoreline migration, and a negative to the opposite. Nourishment adds to the total sediment budget and thereby impacts these trends. For example, a shoreline that was previously retreating may become stabilized. On these timescales, an increase in dune growth may also become noticeable. The impacts of nourishments decrease over time, as the deformation of the nourishment body occurs. Over sufficiently long temporal and spatial scales, the nourishment is diffused in cross-shore and longshore directions. The rate and extent of this diffusion depend on the scale of the nourishment relative to its environment and the hydrodynamic climate. Diffusion is generally stronger when the vertical amplitude of the perturbation is higher, its horizontal wavelength is shorter, and under a highly energetic wave climate (Hamm et al., 2002).

A broad set of complex physics-based models has been applied to study nourishment impacts on the short and medium timescales, for example, XBeach (e.g., Baykal et al., 2017; Huisman et al., 2019), Unibest-TC (e.g., van Duin et al., 2004), Delft-3D (e.g., Giardino et al., 2010) and Cshore (e.g., Kalligeris et al., 2020)These models describe elementary basic processes of flow, waves, and sediment response and have been applied to study how the placement of a single nourishment changes topography, which in turn affects hydrodynamics and thereby morphological evolution. Recently, the timescales that can be reached with these models have increased, and examples exist of morphological forecasts spanning multiple years (Luijendijk et al., 2019; Ranasinghe, 2016). However, their practicability to assess the decadal impacts of repeated nourishment is yet limited as extensive calibration is required. This calibration leads to site-specific parameter settings and process formulations, which in turn can result in inaccurate predictions beyond the calibration/validation period (Montaño et al., 2020; Ranasinghe, 2020). Additionally, the computational effort of process-based approaches is considerably large, further limiting their practicability to test multiple nourishment designs.

Long-term (decades to millennia) coastal behaviour is generally related to a large scale (~10–100 km). It is often described as the gradual adjustment of an entire coastal system to an equilibrium that matches the total sediment budget and (changed) climatic circumstances (Bruun, 1954, 1962). This includes relative sea level variation and changes in storm frequency and intensity. Nourishment programs commonly adopt an equilibrium perspective, wherein the focus lies on the long-term, large-scale viewpoint. In this perspective, the analysis of a nourishment strategy primarily considers the sediment volume added, irrespective of the specific placement location (e.g., McCarroll et al., 2021). Coastal profiles are herein assumed to respond to nourishment by rapid equilibration to a new shape after sand nourishment, suggesting a direct correlation between the amount of nourishment applied, the profile volume, and the coastline. Thus, any short- and medium-term impacts of nourishment on coastal indicators are not covered by this approach. However, when large volumes of sand are added to account for the anticipated acceleration of sea level rise, the shape of the profile can deform substantially. In such instances, equilibrium-type approaches may provide erroneous information regarding the evolution of the shoreline and offer no insight into the beach width variability.

1.2. Problem statement

Understanding the time-varying deformation of the coastal profile is essential for gaining insights into coastal state indicators that are closely associated with nourishment objectives. Such insights can inform strategic decisions pertaining to nourishment projects, including the appropriate volume of sediment to be applied, the expected frequency of nourishment cycles, and the optimal cross-shore location. These considerations encompass not only the direct impacts immediately following nourishment placement but also the long-lasting effects that persist over multiple decades. Nevertheless, currently used modelling techniques fail to effectively integrate the necessary spatial resolution with the required decadal time horizon for conducting such an analysis. Process-based approaches are yet impractical due to demanding computational efforts and extensive calibration needs, while equilibrium-type approaches miss the required level of detail. What we seek is a middle ground, a method that bridges the gap between short- and long-term nourishment modelling. How can we effectively address this gap and comprehend the combined influence of multiple nourishment interventions in a slowly changing environment?

1.3. Bridging the gap between short and long-term nourishment modelling

The answer may lie in an alternative viewpoint that has yet been little explored in the context of nourishment programmes. Given the ever-changing nature of boundary conditions and significant profile deformation due to nourishment on shorter timescales, it becomes evident that a state of static equilibrium is never truly attained in practical scenarios. Instead, a continuous and gradual adaptation takes place towards a ‘dynamic equilibrium’. This ‘dynamic equilibrium’ then refers to a normative average morphology that matches the instantaneous sediment budget and climatologic circumstances and can serve as a reference around which the actual morphology fluctuates. The duration of this adaptation depends on profile depth, ranging from hours in the vicinity of the waterline (e.g., Lippmann and Holman, 1989) to millennia in the proximity of the inner shelf (e.g., Stive and de Vriend, 1995). To what extent the average morphology resembles a dynamic equilibrium relies on this timescale of morphological response with

respect to the timescale and magnitude of the changing boundary conditions. In this context, nourishment acts as one such dynamic boundary condition.

A limited set of models have been built upon this philosophy, that the introduction of a nourishment essentially constitutes a perturbation to a coast, having a particular dynamic state (Chen and Dodd, 2019, 2021; Coelho et al., 2017; Marinho et al., 2017; Stive et al., 1991). Over sufficiently long temporal and spatial scales, this perturbation is diffused in cross-shore and longshore directions. Such an approach was developed by Stive et al. (1991), who used a generic combination of physical inductive concepts and a detailed process-based model to simulate cross-shore dynamics resulting from repetitive beach- and nearshore nourishment. Work building forth on this approach was mostly data-driven (as by Baramiya et al., 2019; Capobianco et al., 1994; Lavrentiev, 2015), resulting in parameter settings and process formulations that limit the forecast horizon to a single nourishment cycle in a specific setting. Examples of other diffusion-type applications are the work of (Chen and Dodd, 2019, 2021), wherein the nourishment dispersion has been calculated based on physics-based equations including wave, tide, and sediment dynamics, or a data-driven sediment-budgeting method applied to a nourishment (Marinho et al., 2017).

To establish a foundation for our study, we build forth on the inductive assumptions on dynamic profile response proposed by Stive et al. (1991). With the execution of more nourishments and the availability of bathymetric profile datasets spanning multiple decades and various sites, there is now an opportunity to combine Stive's methodology with the latest knowledge on long-term nourishment behaviour in a predictive model. To this end, we are introducing a diffusion-type behavioural model named Crocodile (**Cro**ss-shore **Co**astal **Di**ffusion **L**ong-term **E**volution model).

The novelty in our approach is the specification and quantification of the model terms and parameters through the use of inductive ideas inferred from observed or expected behaviour, on the grounds of long-term records of bed level data at nourished coasts. With Crocodile, we present a tool that is simple, robust and computationally efficient, designed explicitly to examine the decadal-scale behaviour of coastal indicators previously used to guide or evaluate nourishment programmes, i.e., coastal volume, coastline position (Brand et al., 2022; Hanson et al., 2002) and beach width (Cabezas-Rabadán et al., 2019; McLachlan et al., 2013; Valdemoro and Jiménez, 2006).

1.4. Paper outline

The paper starts by presenting the theoretical frame of reference for Crocodile (2.1), followed by a model description that details its specific design and implementation (2.2). In this paper, Crocodile is applied on the central Holland coast. We included a description of the relevant morphological and hydrodynamical details of the region and the local nourishment policy (3.1). The model set-up for all simulations is described (3.2), along with varied parameter settings per simulation (3.3). Crocodile is then applied to simulate idealized nourishment strategies (4.1) and to hindcast cross-shore coastal evolution at case study locations with varying nourishment histories (4.2) over a couple of decades. Finally, we discuss the total performance of Crocodile in different cases (4.3) and discuss strengths, limits, and potential applications (5). Finally, the paper concludes (6) by evaluating Crocodile's ability to simulate the temporal evolution of coastal indicators under various nourishment programmes.

2. Methods

2.1. Model philosophy

The present modelling framework builds forth on principles proposed by Stive et al. (1991), wherein the reshaping of the cross-shore profile depend on the vertical magnitude of perturbations to the long-term equilibrium profile as well as the hydrodynamic climate. The novelty in our approach lies in the definition and quantification of the model terms and parameters based on inductive insights as well as decadal records of bathymetry and topography along nourished coasts. Crocodile computes the evolution of the cross-shore profile shape which is then translated to the coastal indicators of interest. The model is behaviour-oriented, meaning that the model components are formulated to optimally simulate the evolution of these indicators without aiming to resolve the underlying physics other than mass-conservation.

We consider sandy beaches with lengths in the order of kilometres, wherein the longshore variation of the coastal profile and hydrodynamic processes can be neglected. As we consider the nourishment as a profile perturbation and assume a 'dynamic equilibrium' background profile, any autonomous (nourishment-independent) profile development affecting the profile shape is not resolved. This means that cycles of storm and recovery, cyclic bar behaviour and the passage of alongshore shoreline undulations are not included.

2.2. Model description

In this section, we present a summary of the mathematical equations that comprise the model. Every timestep t, Crocodile computes the 'instantaneous' bed level $Z(x,t)$ being the time-dependent profile approaching a dynamic equilibrium profile $Z_{eq}(x,t)$. The horizontal coordinate system x is defined positively offshore from the landward model boundary. Two vertical coordinate systems denoted as z and z' are utilized, which are both defined positively upwards from the mean water level (MWL) but originated from different points. While z refers to a vertical position with reference to $MWL(t=0)$, z' is anchored at $MWL(t)$. Both Z and Z_{eq} are defined within the z coordinate system. Changes in the coastal system (e.g., sea level rise, alongshore transport gradients, or the implementation of nourishments) lead to horizontal and vertical translation of $Z_{eq}(x,t)$ as given by a sediment volume balance (see Fig. 1a–d). The translation component of sea level rise is modelled based on the principles established by Bruun (1954, 1962), whereby the equilibrium profile is raised by the change in sea level and shifted onshore to balance total sediment volume.

At its core, the model computes the rate and extent of sediment dispersion as the sum of five components:

$$\frac{d(Z-Z_{eq})}{dt}=\frac{d}{dx}\left\{D(z')\frac{d(Z-Z_{eq})}{dx}\right\}+\varepsilon_D(z)+E(z')+F(Z-Z_{ini})+W(Z-Z_{eq})+\mathrm{Source}(z',t) \quad (1)$$

2.2.1. Cross-shore diffusion

The first and second RHS components of Eq. (1) describe cross-shore diffusion. The first term is a diffusion term that redistributes any perturbation from Z_{eq} in time and space. It resembles the diffusion term by Stive et al. (1991), and similar diffusion terms have been incorporated in other cross-shore modelling approaches (e.g., Baramiya et al., 2019; Capobianco et al., 1994; Davidson, 2021; Lavrentiev, 2015). It includes the depth-dependent coefficient $D(z')$ (with the physical dimension of m^2/day), which represents the average sediment redistribution capacity along the profile and thereby regulates the morphological timescale of response (Fig. 2). Stive et al. (1991) originally derived the shape and magnitude of $D(z')$ by fitting $D(z')$ to approximate nourished and unnourished runs using a process-based profile model (Unibest-TC), covering timeframes ranging from seasons to decades. In Crocodile, we deviate from this approach by adding a formulation for the subaerial losses and by connecting the shape of the diffusivity profile

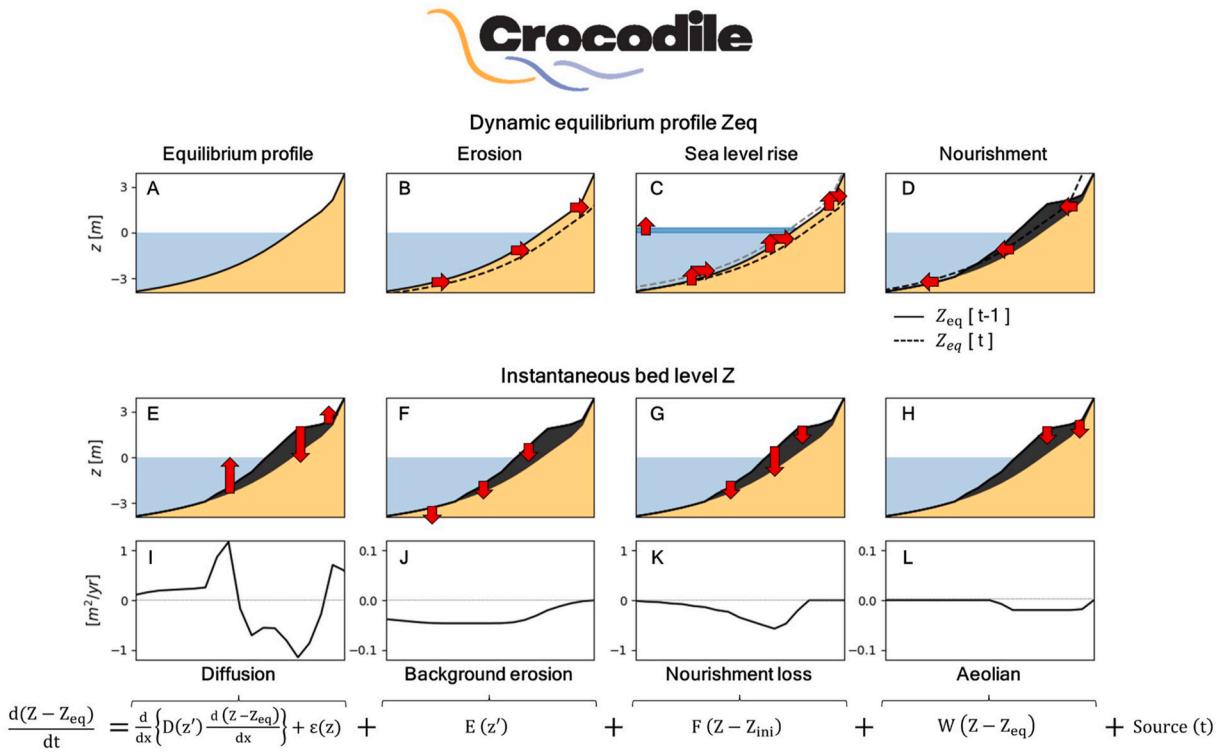

Fig. 1. Schematic overview of Crocodile. Upper row: Translation of the dynamic equilibrium profile (A) as a response to erosion (B), sea level rise (C) and nourishment (D). Red arrows indicate the direction of translation. Middle row: Instantaneous bed level response to nourishment per model subcomponents diffusion (E), background erosion by existing alongshore gradients in transport (F), enhanced alongshore losses at the nourishment (G) and aeolian losses (H). Direction and magnitude of bed level change are indicated by red arrows.
Lower row: Magnitude of model subcomponents as function of the cross-shore position: diffusion (I), background erosion (J), nourishment erosion (K) and aeolian (L) directly after nourishment implementation. Note the different scales.

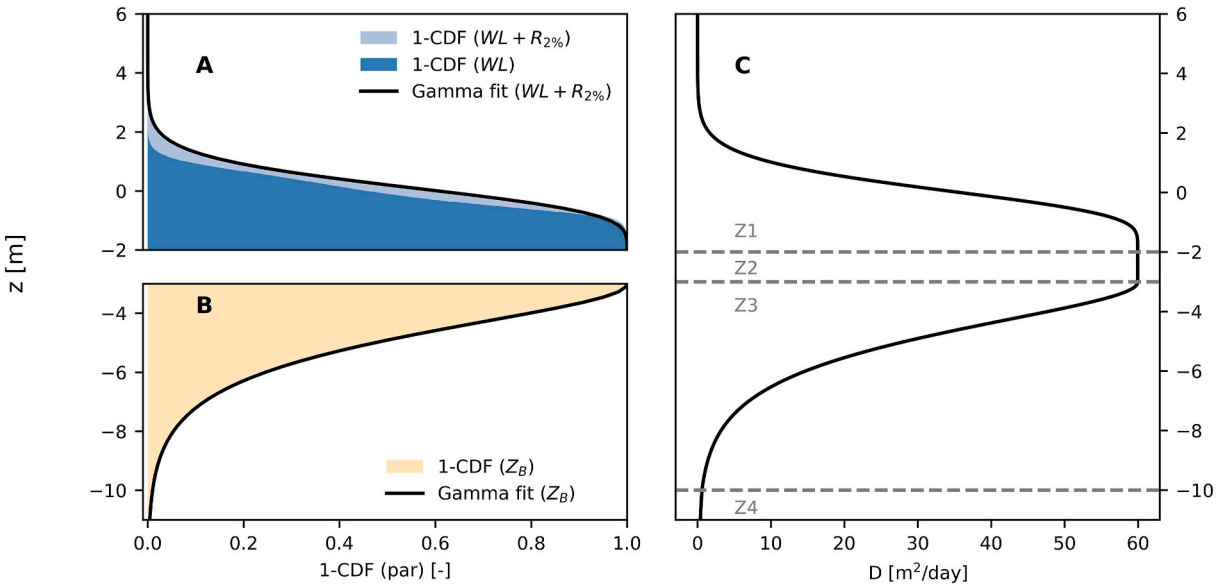

Fig. 2. A) Example survival functions of WL (water level and surge) and $WL + R_{2\%}$ (water level, surge, and wave runup). B) Example survival function of Z_B whereby breaker index γ is set 0.44 (Miche, 1954). C) Resulting diffusion coefficient $D(z')$ with $D_{MAX} = 60\ m^2/day$ as adopted from de Vriend et al. (1993). Z1, Z2, Z3 and Z4 indicate zones as referred to in the main text, divided by the grey dashed lines. The CDFs and zonation in this example are based on the hydrodynamic data of 1985–2018 at the Dutch IJmuiden measuring station.

to the local wave climate. As a result, the submerged part of $D(z')$ closely resembles Stive et al. (1991). The shape of the diffusivity profile $D(z')$ is prescribe ed as a function of boundary conditions and the local hydrodynamic climate, facilitating easy implementation of locations with different hydrodynamic characteristics in Crocodile.

We consider the following morphological zones in the cross-shore profile for defining $D(z')$:

- The upper part of the active zone (Z1 in Fig. 2c), extending from the low waterline Z_{LW} to the maximum elevation reached by wave runup over a decadal timeframe. This zone includes the intertidal area and the subaerial beach, being only recurrently mobilized by wave runup. In this zone, we assume the morphological timescale of diffusion to linearly depend on the frequency that an elevation is reached by wave runup. To estimate this frequency, we adopt a linear relation defined by (Ruggiero et al., 1997) between exceedance elevation for runup maxima $R_{2\%}$ and offshore significant wave height H_s:

$$R_{2\%} = \begin{cases} 0 & for\ H_s < 0.44 \\ 0.5\ H_s\ -\ 0.22 & for\ H_s \geq 0.44 \end{cases} \quad (2)$$

With this relation, we translate a multi-decadal record of the sum of the offshore water level *WL* (including tide and surge) and offshore significant wave height to a survival function (i.e., 1 − *Cumulative Distribution Function*, as visualized in Fig. 2a) that represents the shape of $D(z')$ in this upper zone Z1:

$$\mathrm{D}(z') = D_{MAX} * ((1 - CDF(WL + R_{2\%})) + Z_{LW})\ for\ (Z_{LW} - 1) < \mathrm{z}' \quad (3)$$

Consequently, the diffusion coefficient in the highest zone Z1 is maximum (D_{MAX}) around the (average) low waterline Z_{LW} and decreases to almost zero at the elevation of the extreme total water level. Note that the zone extends 1 m below Z_{LW} to include all area exceeding extreme low water levels.

- A zone of constant maximum sediment diffusivity (Z2 in Fig. 2c) is applied between the low waterline Z_{LW} and the edge of the surfzone during average wave conditions Z_E. This roughly corresponds to the zone of maximum sediment transport identified by De Vriend et al. (1993):

$$\mathrm{D}(z') = D_{MAX}\ for\ Z_E < \mathrm{z}' < (\mathrm{Z_{LW}} - 1) \quad (4)$$

- The lower part of the active zone or surf zone (Z3 in Fig. 2c) where sediment is intermittently mobilized depending on the hydrodynamic conditions. This zone stretches from the average edge of the surfzone Z_E to depth of closure Z_{DOC}. In this zone, we assume wave height to be the primary controlling parameter for the variations in sediment flux over depth (Battjes et al., 1988; Chen and Dodd, 2021). We assume the morphological timescale at profile elevation *Z* here to linearly depend on the water depth of wave breaking $Z_B = -\gamma Z$, whereby γ is set 0.44 (Miche, 1954). To this end, a multi-decadal record survival function of wave height is translated to a survival function and $D(z')$ (as visualized in Fig. 2b), and $D(z')$ is calculated as:

$$\mathrm{D}(z) = D_{MAX} * ((1 - CDF(H_B)) + Z_E)\ for\ Z_{DOC} < \mathrm{z}' < Z_E \quad (5)$$

Consequently, the diffusion coefficient is large in the active zone (zone of maximum wave breaking) and decreases to almost zero at the shoreface (Fig. 2b).

- The lower part of the shoreface (Z4 in Fig. 2c), which is dominated by wave shoaling and tidal currents which is only active at decadal to century timescales. This zone extends from the depth of closure Z_{DOC} to a user defined maximum depth of significant sediment transport Z_{min}. Diffusivity in the lower zone is described as $D(Z_{min}) = D_{dw}/dz' * D(Z_{DOC})$, whereby a gradient of diffusion coefficient in deep water D_{dw}/dz must be estimated. $D(z')$ is assumed to decrease exponentially in between:

$$\mathrm{D}(z') = D(Z_{DOC}) * 10^{\frac{dD_{dw}}{dz} * (z' + Z_{DOC})}\ for\ Z_{min} < \mathrm{z}' < \mathrm{Z_{DOC}} \quad (6)$$

Although many forces and factors that affect morphology and drive morphological change (i.e., bed composition, tidal currents) are not included within these definitions, the most important cross-shore variations in sediment response over the profile are captured within $D(z')$. Key aspects of the formulations are that the morphological timescale is shortest in the zone of maximum wave breaking, and that the edge of the active zone moves seawards if the timescale increases.

Since the diffusion component varies over depth the volume conservation of sand is not guaranteed. To ensure volume conservation, a correction term $\varepsilon_D(z)$ is applied wherein the difference in integrated profile volume ΔVp is redistributed. Hereby, the amount of redistribution per location is weighted by the relative elevation change $dz[t,x] - min(dz[t])$ at that location, whereby parts of the profile that are inactive (i.e., $dZ = 0$) are excluded:

$$\Delta Vp(t) = \int_{t=t-1}^{t=t} \int_{\mathrm{X}=0}^{\mathrm{X}=\mathrm{Xmax}} \left(\frac{\mathrm{d}}{\mathrm{dx}} \left\{ \mathrm{D(z)} \frac{\mathrm{d(Z - Z_{eq})}}{\mathrm{dx}} \right\} \right) dx\ dt \quad (7)$$

$$\varepsilon_D(z) = -dt * \frac{\Delta Vp[t]}{dx} * \frac{dZ[t,x] - min(dZ[t])}{\sum (dZ[t,x] - \min(dZ[t]))}\ where\ dZ[t,z] > 0 \quad (8)$$

2.2.2. Background erosion

The background erosion term $E(z)$ represents sediment supply and losses to the profile through gradients in longshore transport independent of the implementation of any nourishments, with the physical dimension $m^3/m/yr$. Gradients can originate from natural processes and human activities such as engineering works at adjacent beaches. For the sake of simplicity, we keep $E(z)$ constant over time throughout the simulations. Given that the alongshore gradients predominantly occur within the active profile zone, we distribute the volume change over the profile with the shape of $D(z)$:

$$E[z] = E_{tot} * \frac{D(z)}{\int_{Zmin}^{Zmax} (D(z))\ dz} \quad (9)$$

In the current application the magnitude of sediment changes due to ambient alongshore gradients is obtained from a multi-year record of profile elevation changes $dZ_{obs}(x)$:

$$E_{tot} = \int_{Tmin}^{Tmax} \int_{Xmin}^{Xmax} dZ_{obs}(x)\ dxdt$$

Alternatively, E_{tot} could also be estimated using a longshore transport model or coastline data.

2.2.3. Nourishment loss

The third RHS element in Eq. (1), $F(Z - Z_{eq})$, represents the enhanced sediment losses following the implementation of a nourishment. These losses stem from the increased exposure of the new coastline to waves and currents, compared to its neighbouring profiles (Verhagen, 1993). As described by Verhagen (1996) enhanced sediment loss dV_f from initial beach nourishment volume V_{ini} can be described with an exponential decay function:

$$dV_f[t] = -P * V_{ini} * e^{-\frac{t}{\Phi}} \quad (10)$$

Whereby *P* represents the fraction of V_{ini} that is dispersed over the nourishment lifespan and Φ represents a nourishment loss exponent. This means that fraction $(1 - P)$ is covered by the other terms on the RHS of Eq. (1).

The magnitude of the enhanced sediment losses following the implementation of a nourishment has been linked to the wave climate, profile steepness, the active height of the zone with alongshore transport and the extent of the nourishment (Arriaga et al., 2017; Huisman et al., 2013). Considering these dependencies, we assume that Φ increases with depth and we assume that *P* decreases with depth. This depth-dependency offers an advantage, as it allows us to incorporate shoreface nourishments, which were not considered in the analysis by Verhagen (1996). To this end, we define the depth-dependent nourishment loss $dV_{f,Z}(t,z)$ at timestep $(t - t_n)$ after nourishment:

$$dV_{f,Z}[t,z] = -\mathrm{p(z)} * (\mathrm{Z} - \mathrm{Z_{ini}}) * e^{-\frac{t-t_0}{\varphi(z)}} \tag{11}$$

Herein, $p(z)$ and $\varphi(z)$ are the vertically varying counterparts to P and Φ from Eq. (10). V_{ini} has been replaced by $(Z - Z_{ini})$ to account for multiple successive nourishments as well as contemporary profile evolution resulting from the other terms on the RHS of Eq. (1).

In the definition of $\varphi(z)$ we follow the shape of $D(z)$, assuming that the timescale of enhanced nourishment losses in the region permanently submerged ($Z < Z_{LW} - 1$) is linearly dependent on the relative sediment redistribution capacity along the profile (Fig. 3):

$$\varphi(z) = \begin{cases} \varphi_B \ \ for\ Z \geq \mathrm{Z_{LW}} - 1 \\ \varphi_B + \dfrac{d\varphi}{dD} * \dfrac{\mathrm{D_{max}} - \mathrm{D(z)}}{\mathrm{D_{max}}} \ for\ Z < \mathrm{Z_{LW}} - 1 \end{cases} \tag{12}$$

Thereby, φ_B represents the nourishment loss exponent for beach nourishments and $d\varphi/dD$ its increase relative to $D(z')$. Likewise, we assume that the fraction of enhanced nourishment loss is linearly dependent on the relative sediment redistribution capacity along the profile:

$$p(z) = \begin{cases} p_B \ \ for\ Z \geq \mathrm{Z_{LW}} - 1 \\ p_B + \dfrac{dp}{dD} * \dfrac{\mathrm{D_{max}} - \mathrm{D(z)}}{\mathrm{D_{max}}} \ for\ Z < \mathrm{Z_{LW}} - 1 \end{cases} \tag{13}$$

Estimations of both terms can be obtained from either observations or an analytical approach. $F(Z - Z_{eq})$ in Eq. (1), being the rate the enhanced sediment losses following the implementation of a nourishment, is then given by the time derivative of $dV_{f,Z}[t,z]$:

$$F(Z - Z_{ini}) = \frac{dV_{f,Z}}{dt} \tag{14}$$

Due to the volume dependency, $F(Z - Z_{eq})$ is largest directly after nourishment placement and decreases gradually over time.

$F(Z - Z_{eq})$ is particularly large when a nourishment has a feeder-type function. For feeder-type nourishments where planform coastline curvature drives substantial lateral losses, we propose an alternative approach to determine nourishment loss exponent φ following Tonnon et al. (2018). Essential herein is the definition of a longshore transport intensity parameter ($\partial \mathrm{Qs}/\delta\theta$), defined as the variation of the net longshore transport $\mathrm{Qs}[m^3/\mathrm{yr}]$ for a small change of the coastline orientation $\theta[^\circ]$:

$$\frac{\partial \mathrm{Qs}}{\delta\theta} = \frac{\mathrm{Qs}}{\Delta\theta} * \cos(2\Delta\theta) \tag{15}$$

wherein $\Delta\theta[^\circ]$ is the relative difference between the local coastline orientation and the coastline orientation that yields net zero sand transport. Tonnon et al. (2018) propose that φ relates to nourishment design parameters $V_{ini}[m]$ (initial nourishment volume), $L_{ini}[m]$ (initial nourishment length) and $W_{ini}[m]$ (initial nourishment cross-shore width):

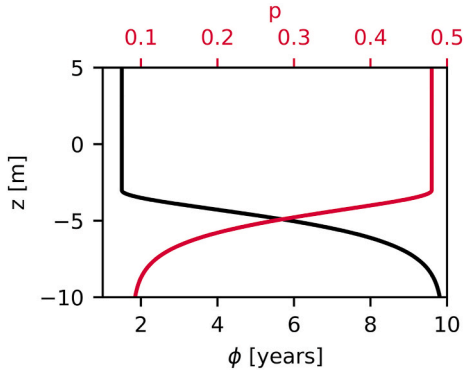

Fig. 3. Variation of p(z) and $\varphi(z)$ with profile elevation z.

$$\varphi = 1.91 * 10^{-2} * V_{ini} * \left(0.2 * \frac{L_{ini}}{W_{ini}} + 1\right) \left(\frac{\partial \mathrm{Qs}}{\delta\theta}\right)^{-1} \tag{16}$$

The constant $1.91 * 10^{-2}$ scales with $\partial \mathrm{Qs}/\delta\theta$ ($30.000\ m^3/\mathrm{yr}/^\circ$ in Tonnon et al. (2018)) and includes the impact of the wave climate, cross-shore profile, and sediment. This φ can be adjusted to other locations by recalculating $\partial \mathrm{Qs}/\delta\theta$ and scaling the constant in Eq. (16). $F(Z - Z_{ini})$ can then be calculated by substituting φ in Eq. (11) with p(z) = 1 and subsequently substituting $dV_{f,Z}$ in Eq. (14).

2.2.4. Sediment exchange with the dune area

The fourth RHS component of Eq. (1), $W(Z - Z_{eq})$, describes variations in sediment exchange from the subaerial beach and the intertidal zone to the dune area (Fig. 1 h, l). If the profile is equal to the equilibrium profile ($Z = Z_{eq}$) the subaerial beach and the intertidal zone are, by definition, in morphodynamic balance. In other words, for $\mathrm{Z} = \mathrm{Z_{eq}}$, the volume of sediment transferred from deep water to the beach balances the long-term landward sediment transfer from the beach towards the dune area. However, this balance does not imply zero dune growth, as a net landward sediment supply can exist within the equilibrium profile (i.e., the equilibrium concept does not include the dune area). $\mathrm{W\ (Z - Z_{eq})}$ thus only represents the change in dune growth with respect to an initial situation. Total dune growth can then be computed by adding $\mathrm{W(Z - Z_{eq})}$ to the initial net landward sediment supply.

On a decadal timescale, dunes evolve in a variety of ways dependent on biological, geological, and physical factors (Carter, 1991). Hence, it is difficult to quantify and predict the impact of nourishment on duneward sediment exchange. However, we can simplify the depiction to highlight some primary anticipated impacts. Several studies have shown that wider beaches may lead to higher sediment supply (Davidson-Arnott and Law, 1996; De Vries et al., 2011) and increased protection against storm wave attack (Davidson-Arnott, 2005). Therefore, we confine our definition of $\mathrm{W\ (Z - Z_{eq})}$ to the critical fetch theory, whereby the amount of aeolian sediment transport linearly scales with fetch length until a certain limit is reached (Bauer et al., 1996). If the beach width exceeds its initial value BW_0, it results in an additional net transport of sediment towards the dune, while a beach width narrower than BW_0 causes the dunes to supply sediment to the beach. The dune area is modelled as a source or sink of sediment, i.e., its type, shape and evolution are not modelled.

We adopt a linear relation between beach width and dune growth in $\mathrm{m^3}$ per m alongshore whereby linear coefficient α must be estimated:

$$W_{calc} = \frac{\alpha}{dt} * (BW - BW_0)$$

Following the critical fetch theory, we assume that dune growth reaches a constant maximum value W_{Max} when a certain critical beach width BW_c is exceeded:

$$W_{total} = \min\left(W_{calc}, W_{max}\right) \tag{16}$$

Whereby,

$$W_{max} = \frac{\alpha}{dt} * (BW_c - BW_0) \tag{17}$$

Sediment that is used to adjust the dune growth is subtracted from (or added to) the intertidal zone and subaerial beach.

$W[Z - Z_{eq}]$ is then subtracted from the intertidal area and subaerial beach:

$$W[Z - Zeq] = \frac{-W_{total}}{X[Z_{df}] - X[\mathrm{Z_{LW}}]} \ for\ Z_{LW} \leq Z \leq Z_{df} \tag{18}$$

Reported relations between beach width and dune growth are highly variable over time and space, as noted by De Vries et al. (2011). The same applies to the magnitude of a critical beach width or a maximum dune growth rate. Nevertheless, the presented approach provides a

system description with a sufficient scientific basis to depict the major aspects of dune growth impacts related to nourishment, wherein dune growth at recently nourished beaches increases with beach width until a certain maximum. In the context of the current application, this comprehensive system description provides an adequate basis to differentiate between nourishment scenarios.

2.2.5. Nourishment implementation

Nourishments are added into dynamic profile Z using the *Source* (z,t) term. For the current study we avoid intricate designs and instead employ triangular cross shore designs, comprising a near horizontal platform and a linear slope towards the nourishment toe (Fig. 1d). The cross-shore added volume V_n and design height H_n (upper connection point to profile Z), landward slope S_{lw} and seaward slope S_{sw} are predefined. Crocodile then computes a shape that matches these four design characteristics.

2.2.6. Computed coastal state indicators

Crocodile returns the 'instantaneous' bed level $Z(x,t)$. Bed level data are translated to three coastal state indicators: the temporal evolution of profile volume change ΔV_p, beach width BW and shoreline migration ΔCL.

$$\Delta V_p = \int_{X_{min}}^{X_{max}} (Z(x,t) - Z(x,t=t_0))\, dx \tag{19}$$

The position of the coastline X_{cl} is determined by calculating a volumetric weighted average between the horizontal positions of high (X_{HW}) and low water (X_{LW}). This involves integrating $Z(x,t)$ between X_{HW} and X_{LW} to obtain the sand volume above the level Z_{LW} in this section. The adoption of this volume-based approach aims to avoid that local small-scale variations in profile height, such as intertidal sand bars, result in large fluctuations in X_{cl}:

$$X_{cl} = X_{HW} + \frac{\int_{X_{HW}}^{X_{LW}} (Z(x,t) - Z(X_{LW},t))\, dx}{2 * (Z_{HW} - Z_{LW})} \tag{20}$$

X_{cl} is used to compute BW and ΔCL, whereby the landward limit of the beach width is positioned at the initial horizontal location of the dune foot $X_{df}(t=0)$.

$$BW = X_{cl}(t) - X_{df}(t=0) \tag{21}$$

$$\Delta CL = X_{cl}(t) - X_{cl}(t=0) \tag{22}$$

BW and ΔCL only differ by their point of reference. We chose to include both variables in our analysis, as ΔCL depicts absolute changes while BW offers insights from a relative perspective.

3. Model application: the holland coast

The Crocodile model is applied to the central Dutch coast in two ways. Firstly, we examine idealized nourishment scenarios to analyse whether Crocodile can replicate corresponding behaviour of coastal indicators (see chapter 4.1). Moving from this conceptual application, we transition to nourished case study sites along the central Dutch coast to examine Crocodile's performance reproducing site-specific behaviour resulting from diverse nourishment strategies using measured profiles (see chapter 4.2.).

3.1. The Holland coast: site description and nourishment strategy

The Holland coast consists of sandy beaches and dunes with an average tidal range of about 1.6 m (Wijnberg and Terwindt, 1995). These beaches are interrupted by various structures, including harbour moles (IJmuiden, Scheveningen, and Hoek van Holland), discharge locks (Katwijk aan Zee), and a sea dike (Hondsbossche and Pettemer Zeewering). The nearshore zone is characterized by a roughly uniform, gradual sloping beach profile, occasionally interspersed with periodic nearshore bars. The shoreface slopes vary alongshore between 1:400 and 1:160, and slopes in the breaker zone vary from about 1:50 to 1:150 (Wijnberg and Terwindt, 1995).

The primary concern driving the current nourishment strategy the Netherlands is safety against flooding. Over time, the total volume of nourished sand has increased to a current level of about 12 million m3 of sand per year. The sand is mainly supplied to the shallow zone (shallower than NAP -8 m) and is not spreading (yet) or only slowly to the deeper coastal zone. This leads to an increase in the average sediment volume in the shallow zone compared to the deeper zone. As a result, the profile of the Dutch coast becomes relatively steeper (van der Spek et al., 2007). The quantity and type of nourishment supplied vary per location and depend on various factors such as the current condition of the beach and dune system, anticipated future changes, and the preferences of local stakeholders. Additionally, some locations receive additional sand to maintain sufficient sediment supply for areas that cannot be nourished. As a result, different nourishment strategies are employed in different locations along the central Dutch coast. For the purposes of this study, three locations have been chosen, each with varying coastal profiles and nourishment histories. From North to South: Egmond, Katwijk, and Monster (Fig. 4).

3.2. Model set-up for all simulations

3.2.1. Profile schematization

This section introduces the profile schematization and sums the parameters used for all simulations. Both $Z(x,t=0)$ and $Z_{eq}(x,t=0)$ are derived from a smoothened multi-year average measured profile obtained from the JARKUS dataset (Wijnberg and Terwindt, 1995). The smoothening and averaging ensure that such that the dynamics of the nourishment are isolated from concurrent coastal behaviour (e.g., cyclic bar behaviour). The beach is extended linearly from the dune foot Z_{df} to the upper model boundary Z_{max}, with the slope equal to the dune slope observed between +4 and + 6 m above sea level. The temporal resolution in the numerical scheme dt is 1/10 year, the spatial resolution in the cross-shore dx is 20 m. The mean water level is set $MWL(t=0) = 0\ \mathrm{m}\ NAP$, NAP being the local Dutch vertical datum, approximately equal to mean sea level. MWL rises linearly throughout all simulations with $SLR = 1.7\ mm/yr$, equal to the average observed relative sea level rise along the Dutch coast over the past century (Drijfhout and Le Bars, 2021).

3.2.2. Parametrization

All hydrodynamic and morphodynamic parameter values are obtained from literature concerning the central Dutch coast (Table 1). Elevations that mark the zonation in the diffusion curve $D(z')$ are based on Wijnberg and Kroon (2002), rounded to $Z_{HW} = 1m\ NAP$, $Z_{LW} = -1m\ NAP$, $Z_{df} = 3m\ NAP$ and $Z_B = -3m\ NAP$. The maximum diffusion coefficient D_{max} is adopted from De Vriend et al. (1993), who estimated that $D_{max} = 60\ m^2/day$ for the central Dutch coast. Offshore wave height and water level statistics used to define the shape of $D(z)$ are obtained from the IJmuiden station of the Dutch Ministry of Public Works, located 35 km offshore (Fig. 4). The gradient of diffusion coefficient in deep water dD_{dw}/dz is taken 1/100 following estimates of morphological timescales for the Dutch coastal shelf from numerical model experiments (Boers, 2005). Any estimate for this gradient is site-specific and arbitrary, however the model results show little sensitivity to this deepest part of the $D(z)$ curve within the current application. A common value for wave breaker index $\gamma = 0.44$ is adopted from Miche (1954). For the Holland coast, Tonnon et al. (2018) estimated $\partial Qs/\delta\theta = 30.000\ m^3/yr/^\circ$ (i.e., $Q_s = 200.000\ m^3/yr$ and $\theta = 6.6^\circ$). The

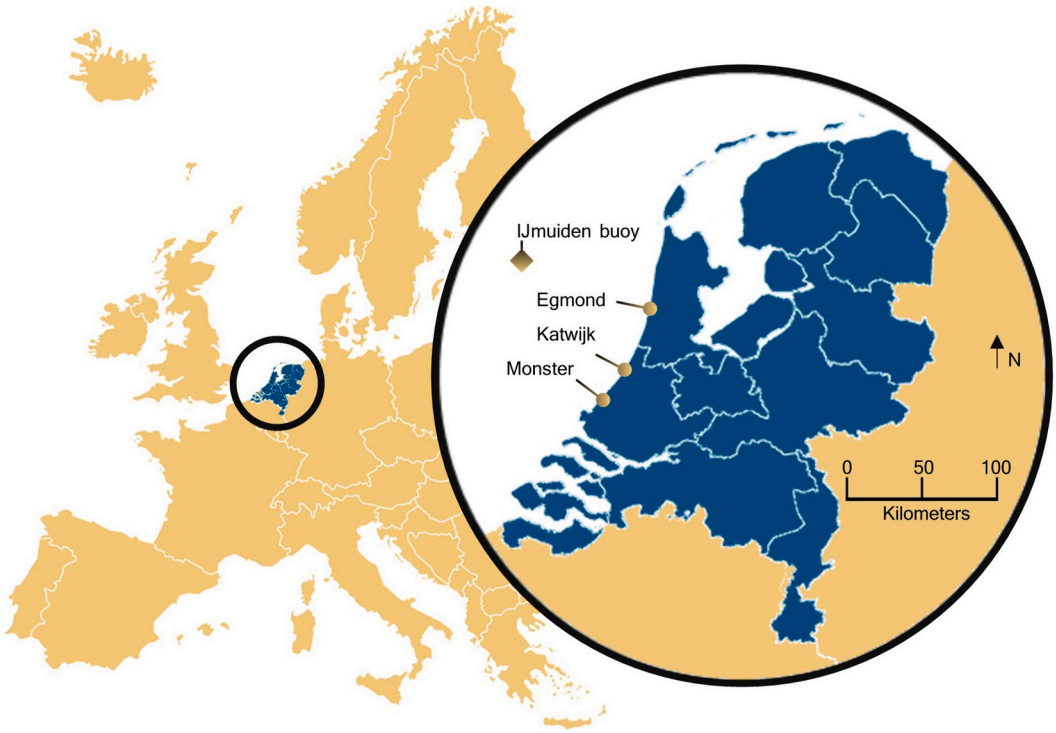

Fig. 4. Locations of case study sites along the sandy Dutch coast and the IJmuiden wave buoy used for the long-term wave data.

linear relation between beach width and dune growth is adopted from de Vries et al. (2012) as $\alpha = 0.1475$, and based on 10-year observations of beach width and dune growth along the Holland coast. Additional dune volume growth W_{Max} is based on the maximum dune growth that has been measured at a mega nourishment in the Netherlands which was 60 $m^3/m/yr$ (Kroon et al., 2022). As the dune growth at adjacent beaches was 15 $m^3/m/yr$, we reason that $W_{Max} = 60 - 15 = 45\ m^3/\ m/\ yr$.

Parameters related to $F(Z - Z_{ini})$ are established through observations of nourishment lifespans based on yearly surveys conducted at multiple nourished locations along the central Dutch coast. These lifespans are defined here as the time that an excess of sand is present in the initial nourishment area compared to the pre-nourished situation. For beach nourishments, we adopt the parameterization of (Verhagen, 1996) who proposed that $p_b = 0.48$ and $\varphi_b = 1.5\ yr$. To define $d\varphi/\ dD$ and dp/dD we use observed nourishment lifespans of shoreface nourishments by Huisman et al. (2019), who studied the cross-shore profile change and alongshore redistribution of 19 shoreface nourishments along alongshore uniform sections of the Dutch coast. On average, 40% ($\pm$ 20% standard deviation) of the initial nourishment volume was eroded from the initial nourishment region after 3 years. From numerical model calculations of initial erosion and accretion rates over these nourishments, Huisman et al. (2019) estimated that on average 27.5% of the eroded sand was redistributed longshore ($\pm$ 12.5% standard deviation). Based on these values, we assume that $p[z = -5m] = 0.275$ and $\varphi[z = -6m] = -\frac{3}{\ln(1-0.4)} = 5.87\ yr$. As $D[z = -2] = D_{max} = 60\ m^2/day$ and $D[z = -6] = 20.7\ m^2/day$, we calculate $d\varphi/dD = \frac{1.5-5.87}{60-20.7} = -0.11\ yr\ m^{-2} day$ and $dp/dD = \frac{0.48-0.275}{60-20.7} = 0.0052\ m^{-2} day$.

3.2.3. Nourishment design parameters

The design height, landward slope, and seaward slope of the implemented nourishments are based on prevalent Dutch values as described by Brand et al. (2022). Hereby we discriminate between beach nourishments, shoreface nourishments and mega nourishments. All have triangular cross shore shapes, comprising a near horizontal platform and a linear slope towards the nourishment toe. For beach nourishments the platform connects with the original profile at $H_n = MSL + 2\ m\ NAP$ .The landward slope is $S_{lw} = 1:200$ and the seaward slope S_{sw} is taken equal to the intertidal slope of $Z_{eq}(x, t = 0)$:

$$S_{sw} = \frac{Z_{HW} - Z_{LW}}{X[Z_{HW}] - X[Z_{LW}]}\ for\ Z_{LW} \leq Z \leq Z_{df} \tag{22}$$

We depart from the latter definition when it becomes impractical to achieve the combination of all four design characteristics. This occurs specifically when there is a combination of a low intertidal slope and low nourishment volume (roughly $V_n \leq 150\ m3/m$). In such situations, we opt for a steeper seaward slope $S_{sw} = 1:20$. Shoreface nourishments are implemented with $H_n = MSL - 4\ m$, $S_{lw} = 1:10000$ and $S_{sw} = 1:50$. Mega nourishments, here defined as nourishment with $V_n \geq 2000\ m3/m$, are implemented with $H_n = MSL + 7\ m$ with S_{lw} and S_{sw} defined similar to those used for beach nourishments.

3.3. Model input per site

Site-specific modifications in the model setup include the record of profile surveys to define the initial profile shapes $Z(x, t = 0)$ and $Z_{eq}(x, t = 0)$ and total background erosion E_{tot}. The nourishment implementation, including its timing, volume, and cross-shore location, can either be predefined or based on certain conditions. For the generic scenarios, nourishments with a predefined volume and cross-shore location are implemented when the shoreline passes landwards of a reference point. For the case studies, all nourishment parameters are predefined according to the local nourishment history.

4. Results

4.1. Idealized nourishment simulations

For our initial analysis, we establish three simulations with nourishment strategies in a Dutch coastal setting. In all simulations, we follow a 'reactive' shoreline maintenance policy. Thereby, a new nourishment is placed when the coastline migrates landward of its initial

Table 1
Parameters that are fixed for all simulations in this research.

Parameter	Description	Value	Source
Parameters used for all simulations			
dt	Temporal resolution	0.1 yr	–
dx	Horizontal grid resolution	20 m	–
Z_{min}	Elevation of lower model boundary	−20 m NAP	–
Z_{max}	Elevation of upper model boundary	20 m NAP	–
$MWL(t = 0)$	Mean water level at t = 0	0 m NAP	–
SLR	Sea level rise	1.7 mm/yr	Drijfhout and Le Bars (2021)
Z_{HW}	Elevation of high water	1 m	Wijnberg and Kroon (2002)
Z_{LW}	Elevation of low water	− 1 m	Wijnberg and Kroon (2002)
Z_{df}	Elevation of dune foot	3 m	Wijnberg and Kroon (2002)
Z_E	Elevation of lower limit of the surf zone during average wave conditions	− 3 m	Wijnberg and Kroon (2002)
Z_{DOC}	Depth of closure	− 10 m	Hinton and Nicholls (1998)
D_{max}	Maximum diffusion coefficient	60 m^2/day	Stive et al. (1991)
$\frac{dD_{dw}}{dz}$	Gradient of diffusion coefficient in deep water	$\frac{1}{100}$	Boers (2005)
γ	Wave breaker index	0.44	Miche (1954)
$\frac{\partial Qs}{\delta\theta}$	Longshore transport intensity parameter	30.000 $m^3/yr/^\circ$	Tonnon et al. (2018)
p_b	Fraction of enhanced nourishment loss	0.48	Verhagen (1996)
φ_b	Nourishment loss exponent	1.5 yr	Verhagen (1996)
$\frac{dp}{dD}$	Gradient of fraction of enhanced nourishment loss	0.0052 m^2day^{-1}	See par. 3.2.2.
$\frac{d\varphi}{dD}$	Gradient of nourishment loss exponent	– 0.11 $yr\,m^2day^{-1}$	See par. 3.2.2.
α	Coefficient of linear relation between beach width and dune growth	0.1475	De Vries et al. (2011)
W_{Max}	Maximum dune growth	$\frac{45\ m^3}{\frac{m}{yr}}$	Kroon et al. (2022)

value, i.e., when ΔCL is negative. The three simulations vary in the cross-shore position and volume of the nourishments applied, with the simulated scenarios being regular beach nourishment, regular shoreface nourishment and mega nourishment. The initial profile and morphological and hydrodynamic model set-up are equal for the three simulations to isolate the impact of the nourishment strategy.

The initial profile applied is a median, smoothened profile based on bathymetric measurements from the unnourished years (1956–1997) at Katwijk beach, the Netherlands. As described by (Huisman et al., 2019), an average observed background erosion rate in the Netherlands is $E_{tot} = -28\ m^3/m/yr$, which is adopted in these generic simulations. The design height and cross-shore shape of the applied nourishments resemble the standard formulations for the different nourishment types described in section 3.2.3. The applied cross-shore nourishment volumes are based on average volumes applied along the central Dutch coast over the past couple of decades as described by Brand et al. (2022), which is $V_n = 200\ m^3/m$ for regular beach nourishments and $V_n = 450\ m^3/m$ for shoreface nourishments. Design dimensions adopted for the scenario with mega nourishments are adopted from Tonnon et al. (2018), reflecting the design of the Sand Engine; $V_n = 9000\ m^3/m$ and $L_{ini} = 1333$. The total simulation duration is 40 years.

The target of the modelling exercise is to analyse whether Crocodile reproduces the evolution ΔV, ΔCl and BW as we expect based on observations. For the beach nourishment scenario, we expect the beach to widen each time a nourishment is implemented followed by rapid erosion, with ΔCl and BW returning to their initial values after about 3 years (Brand et al., 2022). Furthermore, we anticipate observing a disparity in sediment transport rates along the profile, whereby the middle and lower shoreface cannot keep in pace with the upper part of the profile (as observed by van der Spek et al., 2007). This leads to a volume deficit compared to Z_{eq} in these regions. Consequently, ΔV averaged over a nourishment lifetime is expected to decrease progressively. For the shoreface nourishment scenario, the influence of shoreface nourishments on ΔCl and BW is anticipated to have a delayed effect compared to the time of nourishment application. In an evaluation of shoreface nourishments for the central Dutch, Witteveen&Bos (2006) found that the volume in the beach and upper nearshore zone is increased by approximately 10% of the nourished volume after one year and this will further increase up to 20–30% in the years after. After 4–10 years, the nourishment has no effect anymore. The mega nourishment is expected to show similar, but extended characteristics as the beach nourishment scenario with a volume deficit compared to Z_{eq} around the depth of closure.

In all scenarios (Fig. 5), the features described in section 4.1 are generally well reproduced, indicating that Crocodile can effectively simulate profile responses characterizing nourishment application. For the beach nourishment scenario, ΔCl and BW return to their initial values after 3.5 years on average. This return period gradually increases over the simulation from 2.5 to 3.9 years due to sediment piling up on the subaerial beach area. As expected for this scenario, ΔV averaged over a nourishment lifetime decreases over time. By the dissipation of the 9th beach nourishment after 32 years, ΔV has decreased by $-48\ m^3/m$ compared to the initial situation. For the shoreface nourishment scenario, we observe delayed and less distinct effects of the nourishment on ΔCl and BW, aligning with our initial expectations. Both fluctuate with only a 10 m amplitude, reaching maxima at 2.3 years after nourishment implementation. Throughout the simulation, ΔCl and BW take on average 10.8 years to revert to their initial values, which is somewhat slower than the timeframe of 4–10 years reported by (Witteveen&Bos, 2006). The mega nourishment scenario shows similar characteristics as the beach nourishment scenario but with extended spatial and temporal scales. ΔCl and BW increase by 840 m after implementation and return to their initial values after 40 years

4.2. Case studies

The model is applied to three case study sites along the central Dutch coast that vary in coastal profile and nourishment history. For case study site #1 Monster beach we demonstrate the workflow in detail, the other two are presented more concisely. The transect near Monster Beach is examined because it has been subjected to different nourishment strategies, which have resulted in distinct responses of the coastal state indicators. The second case study, Egmond, adopted a strategy of frequent regular small-scale beach nourishments, while the third site, Katwijk, employed a strategy with solely shoreface nourishments.

For each case study, the initial profile shape and total background erosion E_{tot} are obtained from JARKUS profile bathymetric measurements over an unnourished period. As the wave climate shows little spatial variation along the central Dutch coast, hydrodynamic parameter settings are identical. Nourishment application in the model matches the nourishment history of the case study location in volume, timing, and cross-shore position. The objective of the modelling exercise is to analyse to what extent Crocodile replicates observed site-specific morphological responses to nourishment application. The comparison

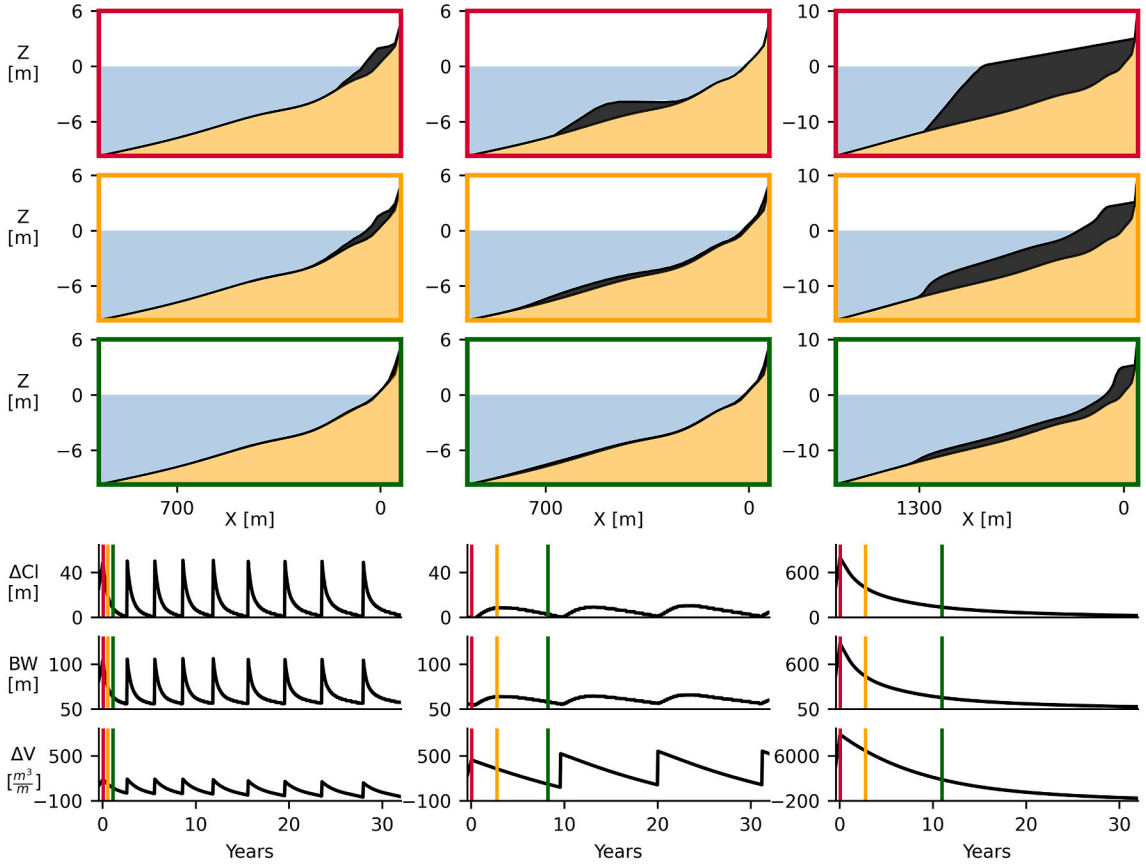

Fig. 5. Demonstration of simulated nourishment scenarios, whereby beach (left), shoreface (centre) or mega (right) nourishments were reactively implemented when ΔCl passed its initial position. The upper three rows display the simulated nourishment evolution at timesteps indicated by the colour of the frames in the lower three rows, that show the temporal evolution of ΔCl, BW and ΔV. The peaks in ΔV and the corresponding responses in other indicators arise from the implementations of individual nourishments.

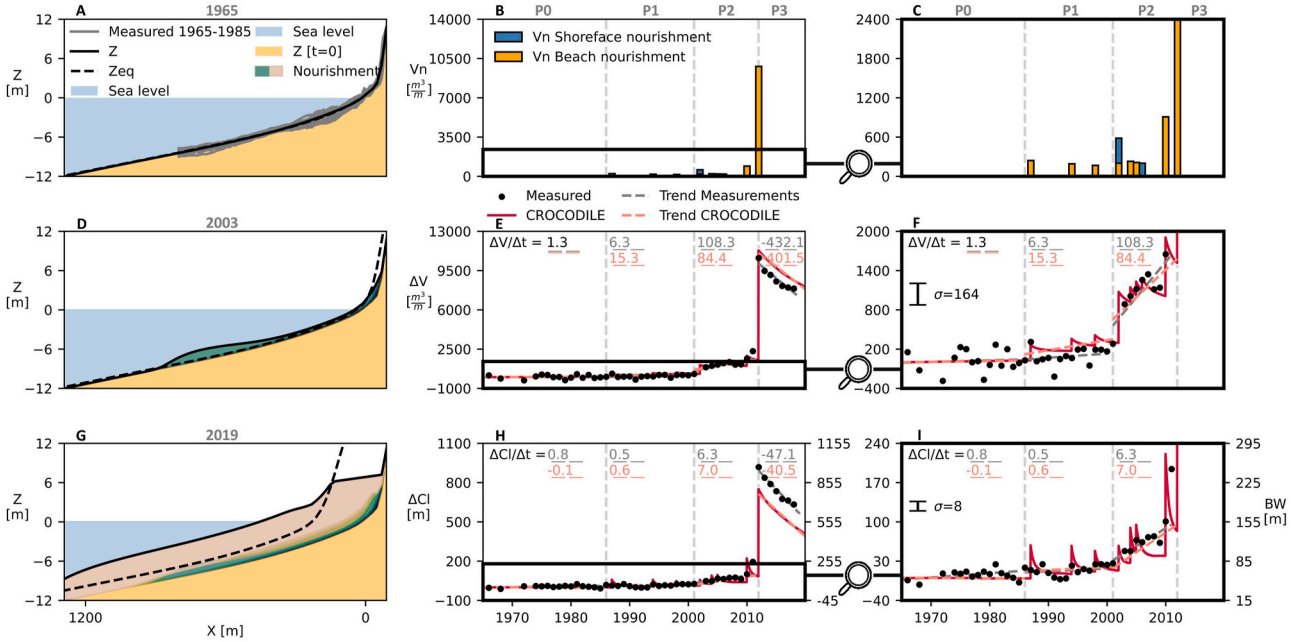

Fig. 6. Left) Snapshots of simulations at the Monster transect. Centre and right) Applied nourishment volume over time, and coastal indicator response, whereby the right plots are a vertical stretch from the black square in the centre plots. Grey dashed lines indicate measurement trendlines, red dashed lines indicate simulation trendlines with rates displayed on top. Trendlines are calculated over the different subperiods (P0–P3), which are indicated on top of 6 B and 6C. A standard deviation for the measurements is indicated with σ.

includes not only absolute values but also trends and trend reversals in these indicators. By focusing on trends, the comparison becomes more straightforward as observations reflect stochastic aspects of hydro-climatic forcing that are not reproduced by the model, which is stationary forced.

4.2.1. Monster beach case study

The transect near Monster beach is examined because it has been subjected to diverse nourishment strategies, The first nourishment conducted in the selected transect was a beach nourishment in 1986. This nourishment was followed by beach nourishments in 1993 and 1997, with the primary objective of preserving the coastline seaward from its 1990s location. From 2001 onwards, it was decided that also sand loss lower in the profile was to be compensated. Consequently, the total nourished volume increased from about 40 $m^3/m/yr$ between 1986 and 2001 to 230 $m^3/m/yr$ between 2001 and 2011 (Fig. 6c). Shoreface nourishments were also introduced during this period. In the JARKUS annual profile measurements, we observe a significant increase ΔV of 108 $m^3/m/yr$ and seaward coastline migration with 6 $m/\ yr$ between 2001 and 2011 (Fig. 6f). In 2011, a 21.5 Mm3 mega nourishment known as the Sand Engine was implemented as a pilot project to test the effectiveness of mega feeder nourishments (Stive et al., 2013) (Fig. 6b).

In our analysis we divide the nourished period in three subperiods; a period of beach nourishment between 1986 and 2001 (P1), followed by a period with more volume supplied in both beach and shoreface nourishment (P2) and the period after the construction of the Sand Engine in 2011 (P3). Crocodile accurately reproduces the long-term pattern of coastal indicators observed during both the nourished and unnourished periods, as depicted in Fig. 6. In the pre-nourished period (P0), both ΔV and ΔCl exhibit relative stability, aligning well with the observed data. It is worth noting that the model simulates a minor retreat of the coastline, which can be attributed to the slight rise in sea level. Between 1986 and 2001 (P1) ΔCl remains stable conform to observations, while the increase in ΔV is overestimated by 9 $m^3/\ m/\ yr$. In contrast, the accretion between 2001 and 2011 (P2) by 108 $m^3/\ m/\ yr$ was underestimated by 12%, and contemporary coastline accretion is accurately reproduced. Thus, regarding the reversal in volume trends following the shift in nourishment strategy, the transition from P0 to P1 was overestimated by 9 $m^3/m/yr$, whereas the transition from P1 to P2 was underestimated by 33 $m^3/m/yr$ (Table 2). Additionally, the reversal in coastline trends after both transitions was well reproduces, with a slight overestimation of 1 m/yr.

The sand engine implementation results in a modelled overestimation of ΔV by 6% and underestimated in ΔCl by 17%. The volume discrepancy results from a disparity between the reported nourishment volume (8995 m^3/m) and the actual volume increase (8306 m^3/m) at the location during the initial JARKUS measurement, which occurred 8 months after the sand engine construction. Over this period, approximately 800 m^3/m of nourishment had already eroded from the transect (De Schipper et al., 2014). The smaller beach width observed can be attributed to the simplified geometry of the sand engine in the simulation compared to its real-world counterpart. In reality, a small lake is present at the location of the transect. As we chose to adhere to the reported nourishment volumes and a simplified geometry, the omission of this lake resulted in a narrower beach width. Lastly, the erosion of the sand engine is slightly underestimated in both ΔV by 31 $m^3/m/yr$ and ΔCl by 7 m/yr.

4.2.2. Egmond aan Zee beach case study

The Egmond aan Zee case study (Egmond from hereon) was examined due to its exceptionally high frequency of (16) nourishments since 1991 (Fig. 7a). We analyse if the effects of a short nourishment return period could be replicated using Crocodile. The major reason for the high nourishment frequency in Egmond is the maintenance of a coastline that is placed seawards compared to adjacent regions, in order to protect the local boulevard. Between 1991 and 1998, six beach nourishments ranging from 120 to 300 m^3/m were carried out. It has been reported that the accumulation of sand from these consecutive nourishments led to relatively fast dissipation of the nourished sand (van der Spek et al., 2007). For this reason, a combination of a shoreface nourishment and a beach nourishment was implemented in 1999 to extend the required return period. As this was successful, in the years hereafter more combinations of beach and shoreface nourishments were implemented with return periods ranging from 3 to 5 years.

A summary of the case study observations and simulated coastal indicators at Egmond is given in Fig. 7c and e. During the unnourished period (P0), $\Delta V/\Delta t$ is by definition reproduced. Over the nourished period (P1), $\Delta V/\Delta t$ increased by 42.5 $m^3/m/yr$ according to JARKUS measurements. This increase is closely replicated with the model, as it was estimated only 4% too high (+44.5 $m^3/m/yr$), The simulated individual nourishment responses to ΔV after 1999 exhibit a sawtooth-shaped pattern resembling the observed data. Over the unnourished period, Egmond showed minimal coastline migration which aligns closely with the observed data (Fig. 7e). During the frequently nourished period from 1991 to 1998, we observe that the seaward migration of the coastline is overestimated (Fig. 7c). Despite ΔV being consistent with observations, Crocodile underestimates the redistribution of the nourished sand in the cross-shore direction, resulting in an excess of sand

Table 2
Measured and simulated trends and trend reversals (noted in the bold arrows) over the specified nourishment timeframes. The error (modelled trends extracted from observed trends) is given in grey. The values under comparison are enclosed in grey dashed circles, accompanied by the percentage of the error relative to the preceding trend reversal (in absolute terms).

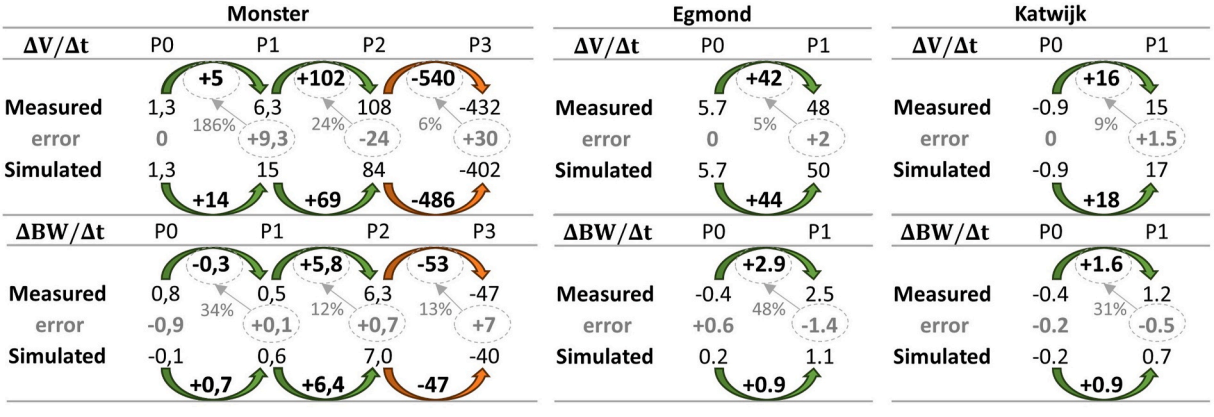

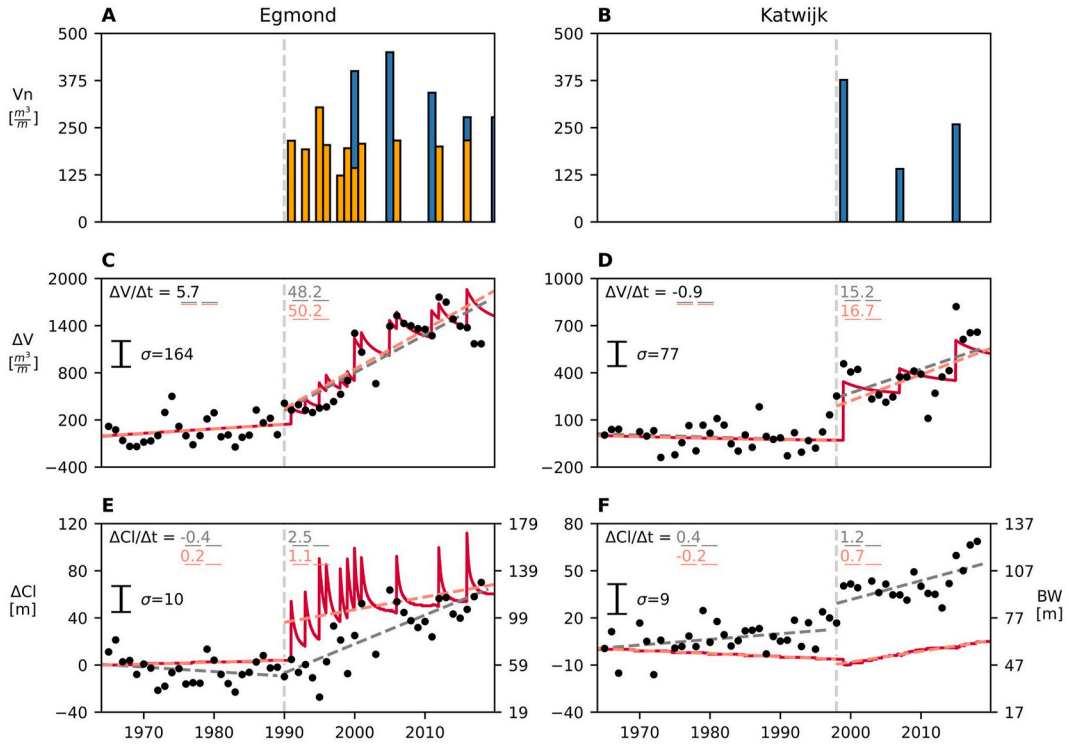

Fig. 7. Observations and Crocodile simulations and at (left) Egmond and (right) Katwijk. A/B) Applied nourishment volume over time. Beach nourishments are orange, shoreface nourishments are blue. C/D) Profile volume. E/F) Coastline migration and beach width. Grey dashed lines indicate measurement trendlines, red dashed lines indicate simulation trendlines with rates displayed on top. A standard deviation for the measurements is indicated with σ.

remaining in the initial nourished area. However, from 1999 onwards, the simulated coastline aligns more closely with the observations. Overall, the rate of change in coastline position ($\Delta Cl/\Delta t$) is underestimated by 56% over the entire period P1, with the sidenote that the overall change in coastline position (ΔCl) is well reproduced.

4.2.3. *Katwijk beach case study*

As an example of a shoreface nourishment strategy, the Katwijk aan Zee case study (Katwijk from hereon) is examined. At the examined transect both the coastal volume and the coastline were fairly stable ($< -1\ m^3/m/yr$ and $< 1\ m/yr$ respectively) until the first nourishment in 1999 (Fig. 7d–f). Nevertheless, the desired coastline was then decided to be shifted seawards to increase protection, as the hinterland has an important societal and economical value. Therefore, the total applied nourishment volume was larger than the local sediment demand. In total, three shoreface nourishment projects were carried out at the Katwijk transect (Fig. 7b). For all projects, we observe that the volume increase measured over the active profile is equal or larger than the volume of nourishment administered. The coastline has moved gradually seawards during the nourished period at a rate of $0.7\ m/yr$. In 2019, a beach nourishment was placed in the area until 250 m North of the investigated transect was placed to mitigate erosion of the coastline. It is unclear whether this adjacent nourishment affected the coastal indicators in the transect, and the period after 2019 is therefore not considered in the analysis.

A summary of the case study observations and simulated coastal indicators at Katwijk is given in Fig. 7. During the unnourished period (P0) $\Delta V/\Delta t$ is again reproduced (Fig. 7D). Over the nourished period (P1), the increase in $\Delta V/\Delta t$ is closely replicated, whereby it was estimated 9% too high. However, the simulations show sawtooth-shaped responses in ΔV following shoreface nourishments, although such behaviour is not clearly discernible in the observations. This demonstrates the nature of Crocodile, where the absence of stochastics leads to an overestimation of the distinctiveness of a nourishment response. Therefore, it can be concluded that while the trend $\Delta V/\Delta t$ is well represented for shoreface nourishment scenarios, the individual response of ΔV per nourishment is overestimated in the model.

Over the unnourished period, our simulation indicates a marginal shoreline retreat of $-0.4\ m/yr$ during the unnourished period, in contrast to the slight accretion observed in the measurements (Fig. 7f). Presently, the formulation used in Crocodile is unable to account for the combination of background erosion and an advancing shoreline. As a result, ΔCl is underestimated over the nourished period at Katwijk. Although the trend reversal as a response to shoreface nourishment is replicated in the simulation, it is underestimated by 42%.

4.3. *Combined results*

Our objective was to present a model approach to evaluate nourishment strategies by simulating the decadal-scale response of repetitive nourishments to key coastal indicators. In this section, we combine the findings of application of Crocodile to Egmond, Katwijk, and Monster to evaluate whether the model successfully simulated these indicators, including trends and trend reversals that coincided with the timing and magnitude of changes in nourishment strategy. Firstly, we examine yearly averages of the simulated coastal indicators and compare these to the yearly observations, as presented in Fig. 8. The modelled and observed coastal indicators show overall good agreement. Specifically, on average (median), the model overestimates ΔV compared to the measurements by 12% (Fig. 8a), while ΔCl and BW are underestimated by 13% (Fig. 8c). These findings validate that the reproduced coastal indicators fall within the appropriate range, which is essential for employing the model as an investigative tool to explore nourishment responses at these sites.

To explicitly assess whether we can simulate coastal response to changes in nourishment strategies, we conduct a comparative analysis of the simulated and measured trends between the specified nourishment timeframes. Within these timeframes, observed $\Delta V/\Delta t$ ranges from $-$

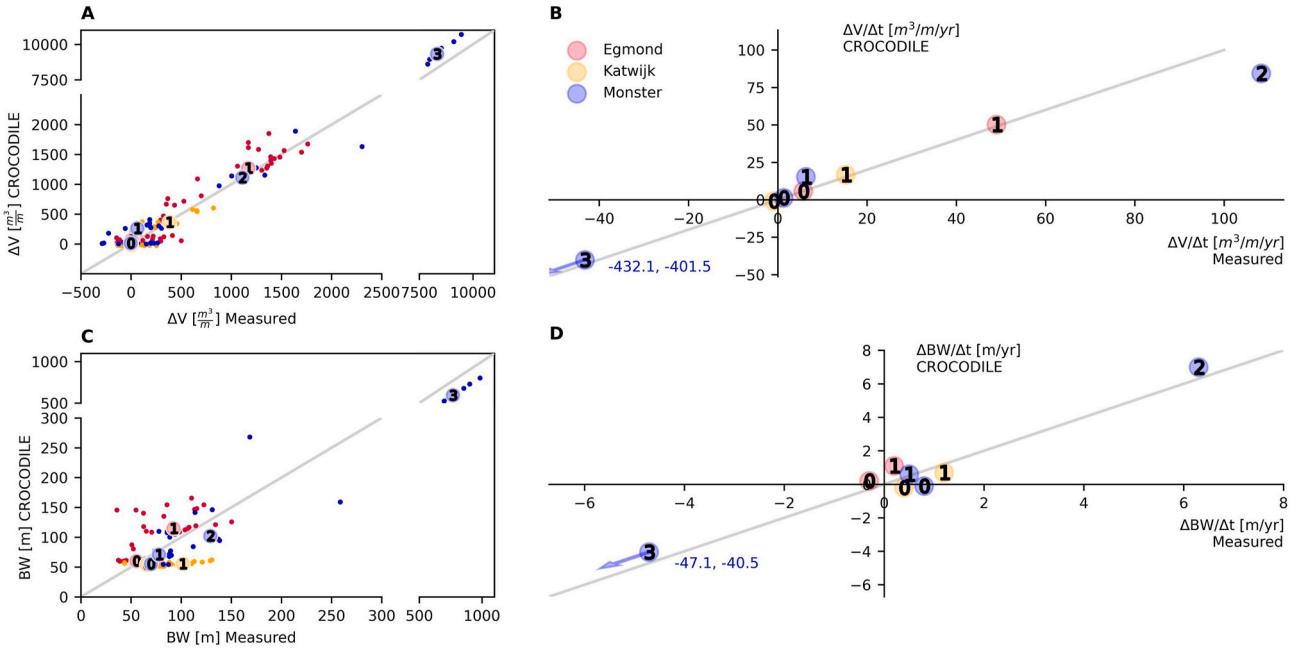

Fig. 8. A/C Measured coastal indicators versus simulated coastal indicators. B/D Temporal trends in measured coastal indicators versus trends in simulated coastal indicators. The big dots show averages over specified nourishment timeframes, whereby the period succession (as displayed in Figs. 6 and 7) is noted by the number in the dot. The blue arrows in panel B/D indicate the direction of the last period at Monster, which lies beyond the plotting area. For all panels, the grey line indicates where these relations fit 1:1. Note that the axes in panels A/C are split to show both beach/shoreface datapoints and mega nourishment datapoints.

432 to 108 $m^3/m/yr$, and observed $\Delta BW/\Delta t$ ranges from −47 to 6.3 m/yr. On average, modelled $\Delta V/\Delta t$ is found to be 1.5 $m^3/m/yr$ (7%) higher than the actual value (Fig. 8b), while modelled $\Delta BW/\Delta t$ is 0.2 m/yr (15%) lower (Fig. 8d). The median reversals in these trends between these intervals are slightly better replicated than the absolute trends. Specifically, we observed a median 2.0 $m^3/m/yr$ (4%) overestimation in trend reversals for $\Delta V/\Delta t$, and a 0.6 m/yr (9%) overestimation in trend reversals for $\Delta BW/\Delta t$.

We consider the trend reversals as indicative of the dynamic profile response to different nourishment periods. Their magnitude can therefore serve as a reference for interpreting the significance of the error in trends between simulation and measurement. This allows us to gauge the relevance of the error when utilizing the model for nourishment strategy evaluations within a specific case study. For instance, in Egmond we observed a volumetric trend of 5.7 $m^3/m/yr$ over an unnourished period, which was increased to 48 $m^3/m/yr$ over the nourished period (Table 2). The model predicted an increase in volumetric trend of 50 $m^3/m/yr$. Comparing the difference between these two to the difference between the observed trends in the two periods shows that the model error is small enough to replicate the response to nourishment. By comparing the difference between these two values (2 $m^3/m/yr$) to the difference between the observed trends in the two periods (42 $m^3/m/yr$), we can deduce that the model error is sufficiently small to discriminate the profile response to nourishment.

When we extend this comparison to encompass all chosen subperiods and various study sites, we consistently observe that all trend reversals exhibit the correct direction (positive/negative). Furthermore, for all but one of the selected subperiods, the magnitude of the trend reversal between a period and the preceding one exceeds the margin of error between simulation and measurement. In Table 2, this comparison is illustrated by the grey arrows accompanied by the percentage of the magnitude of error compared to the preceding trend reversal. This can also be seen in Fig. 8 b/d, by comparing the difference in trend between the subperiods with the distance to the 1:1 grey line. The exception where the error exceeds the trend reversal is the trend change between time period P1 and P2 at Monster beach. In this period, the total amount of nourishment applied was relatively modest, and it is reasonable to deduce that the corresponding minor trend reversal predominantly signifies natural variability rather than being attributable to a response to nourishment. This underlines that Crocodile is able to replicate coastal response to changes in nourishment strategies if this response is large enough and thereby clearly discernible in the observations. Overall, these findings suggest that the model's error is acceptably small compared to the response of the indicators to nourishment, allowing us to confidently assert that the model performs satisfactory for the chosen cases.

5. Discussion

Our objective was to present a model approach to evaluate nourishment strategies by simulating the decadal-scale response of repetitive nourishments to coastal volume, shoreline position and beach width. The model is behaviour-oriented, meaning that the model components are formulated to optimally simulate the evolution of these indicators without delving into the intricacies of underlying physics. Thereby, we intentionally designed the model with simple formulations to enable the decadal simulation of nourishment strategies without extensive calibration efforts. We opted for a purely cross-shore approach, simplifying our analysis by assuming that longshore variations in coastal profiles and hydrodynamic processes along the shoreline can be disregarded for our current purpose.

While Crocodile's strength lies in its simplicity, it also serves as the primary source of its constraints. As we consider the nourishment as a profile perturbation and assume a 'dynamic equilibrium' background profile, any autonomous (nourishment-independent) profile development affecting the profile shape is not resolved. This means that cycles of storm and recovery, cyclic bar behaviour and the passage of alongshore shoreline undulations are not included in the model. In many instances, it can be challenging to discern the effects of nourishment in the observations, especially when there are substantial autonomous coastal developments. Additionally, the observations reflect stochastic aspects of hydroclimatic influences (e.g., energetic vs moderate years) that the model, being stationary forced, cannot replicate. In other words, the

model's outcomes represent the 'climatology' of the simulated coast and provide the anticipated 'annual average' value for a given coastal indicator at a particular time. Consequently, the model cannot be utilized as a predictor or compute specific details of the cross-shore profile shape on short timescales. Instead, its primary capability lies in comparing the long-term profile responses between periods with and without nourishment.

Our study confirmed that the model was able to accomplish this task, as evidenced by the accurate reproduction of trends and trend reversals between the observations and simulations. By focusing on these trends, we effectively bridged the inherent disparity between the observations and simulation results. We selected case study locations for our analysis where we did not anticipate autonomous (longshore) profile development to overshadow the response to nourishment. For future applications, the model formulations (eqs. (2)–(18)) can be refined by using more complex formulations including additional hydrodynamical and morphological processes, if either the study site or modelling exercise requires this. Additionally, we anticipate that integrating Crocodile with a longshore model could facilitate the analysis nourishment applications in longshore non-uniform coastal settings.

Some considerations should be made regarding the selection of input parameters. The parameter values chosen for this study serve as an initial approximation for the Dutch coast. Parameter values (Table 1) are not universally applicable or may change in the future. When applying Crocodile in a different coastal setting, careful evaluation of these parameters is necessary. Furthermore, it is important to acknowledge that the input parameters specific to the case study are sensitive to errors in cross-shore measurements. In the present application, the temporal and spatial resolution were relatively high, but this sensitivity may become more significant when limited measurements are available. Although Crocodile is thought to be transferable to other sandy coastal environments with varying cross-shore profiles and wave climates, it is worth mentioning that this assumption is yet to be verified.

6. Conclusions

A diffusion based cross-shore model, Crocodile, has been developed to simulate the effects of nourishment strategies on coastal indicators such as coastal volume, coastline position and beach width over a decadal timeframe. The model contains elements to compute cross-shore diffusion, sediment exchange with the dune and longshore sediment losses, whereby enhanced lateral loss after implementation of the nourishment is discriminated from 'background erosion'. Crocodile was applied to a series of idealized nourishment scenarios, showing that the model can simulate expected profile responses that characterize nourishment application. Moreover, the model was applied to multiple case study locations along the Dutch coast that have undergone different nourishment strategies over the past decades. Our analysis involved a comparison between annual field measurements at these locations and the model's outcomes, demonstrating a strong alignment. Specifically, the model exhibited a 12% overestimation in profile volume compared to the measurements, while it underestimated beach width by 13%. These findings validate that the reproduced coastal indicators fall within a small range, essential for employing the model as an investigative tool to explore nourishment responses at these sites.

To assess the impact of nourishment strategies on coastal indicators in these case studies, we segmented the observation timeframe into subperiods characterized by variations in nourishment strategies (i.e. nourishment type and volumes applied). Within these subperiods, we computed trends in total profile volume and beach width for both the field measurements and simulation results. Considering all subperiods, observed volume trends ranged from -432 to $108\,m^3/m/yr$ and observed trends in beach width ranged from -47 to $6.3\,m/\,yr$. The median simulated volume trend was found to be $1.5\,m^3/m/yr$ (7%) higher than the measured value, while median temporal beach width trend is $0.2\,m/yr$ (15%) lower. We considered the reversals in these trends between subperiods as indicative of the dynamic profile response to different nourishment periods. These were slightly better replicated than the absolute trends. Specifically, we observed a median $2.0\,m^3/m/yr$ (4%) overestimation in volume trend reversals, and a $0.6\,m/yr$ (9%) overestimation in beach width trend reversals. Thereby, we consistently observed that all modelled trend reversals exhibit the correct sign (positive/negative). We used the magnitude of these trend reversals as a reference for interpreting the significance of the error in trends between simulation and observations. Doing so, we observed that for most of the selected subperiods, the magnitude of the trend reversal between a period and the preceding one exceeded the margin of error between simulation and measurement. This indicates that the model's error is small enough to discriminate the response of the coastal indicators to the different nourishment periods.

These results show that Crocodile successfully simulated the magnitude of key coastal indicators, as well as their temporal trend and trend reversals that coincided with the timing and magnitude of changes in nourishment strategy. Thereby, Crocodile fills a gap left by previous modelling techniques, which often focus on a single spatio-temporal scale and fail to capture the combined effects of cross-shore deformation over a decadal timeframe. Crocodile is relatively simple, robust, and computationally efficient, allowing for multiple (stochastic) simulations to be conducted within a short timeframe. Therefore, Crocodile can facilitate the evaluation of future nourishment strategies, steered by different sea level rise scenarios.

CRediT authorship contribution statement

Tosca Kettler: Conceptualization, Data curation, Investigation, Methodology, Software, Visualization, Writing – original draft. **Matthieu de Schipper:** Conceptualization, Funding acquisition, Methodology, Project administration, Supervision, Writing – review & editing. **Arjen Luijendijk:** Conceptualization, Supervision, Writing – review & editing.

Declaration of competing interest

The authors declare that they have no known competing financial interests or personal relationships that could have appeared to influence the work reported in this paper.

Data availability

Model code is available upon request from the author. The annual coastal data of the Dutch coast is available through https://publicwiki.deltares.nl/display/OET/Dataset%20documentation%20JarKus.

Acknowledgements

The work is funded through the Netherlands Organisation for Scientific Research (NWO) research programme 'CSCAPE: Sandy strategies for sustainable coastal climate change adaptation' (grant number 17595).

A. Case study details

Table A1
Overview of selected sites and corresponding E_{tot} and nourishment history.

Site	Jarkus	E_{tot} [m^3/m/yr]	Nourishments applied				
			Start project Yr - M	End project Yr – M	Type (B/S/M)	Volume (total) [m^3 /m]	Volume/m [m^3/m]
Monster	9,010,920	1.3	1986–05	1986–10	B	1.900.000	241
			1993–06	1993–07	B	1.143.000	191
			1997–01	1997–12	B	834.000	167
			2001–03	2001–11	S	2.970.879	583
			2001–04	2001–05	B	801.178	200
			2003–09	2003–11	B	1.252.797	229
			2004–05	2004–06	B	1.155.951	212
			2005–10	2005–11	S	882.056	200
			2009–07	2010–07	B	5.000.000	909
			2011–03	2011–10	M	17.000.000	8.995
Egmond	7,003,800	5.7	1990–05	1990–05	B	323.318	216
			1992–09	1992–11	B	69.225	73
			1992–05	1992–11	B	1.472.640	120
			1994–06	1994–06	B	106.343	304
			1995–05	1995–05	B	306.000	204
			1997–05	1997–05	B	314.000	123
			1998–06	1998–07	B	244.442	196
			1999–04	1999–04	B	214.515	143
			1999–06	1999–09	S	880.100	400
			2000–06	2000–07	B	207.445	207
			2004–06	2004–11	S	1.800.699	450
			2005–04	2005–05	B	486.023	216
			2011–03	2011–04	B	400.000	200
			2015–07	2016–09	S	2.500.000	278
			2015–04	2015–04	B	432.500	216
			2019–07	2019–09	S	2.500.000	278
Katwijk	8,008,850	−0.9	1998–09	1999–02	S	753, 338	377
			2006–03	2006–09	S	105.503.5	141
			2013–10	2014–03	S	2.200.000	259

References

Arriaga, J., Rutten, J., Ribas, F., Falqués, A., Ruessink, G., 2017. Modeling the long-term diffusion and feeding capability of a mega-nourishment. Coast Eng. 121, 1–13. https://doi.org/10.1016/j.coastaleng.2016.11.011.

Baramiya, D., Gorbenko, N., Lavrentiev, M., Spigler, R., 2019. Diffusion model to predict coastal profile evolutions. OCEANS 2019 - Marseille, OCEANS Marseille 2019 2019-June. https://doi.org/10.1109/OCEANSE.2019.8867524.

Battjes, J.A., 1988. Surf-Zone Dynamics. Annu Rev Fluid Mech 20, 257–291. https://doi.org/10.1146/annurev.fl.20.010188.001353.

Bauer, B.O., Davidson-Arnottt, R.G., Nordstrome, K.F., Ollerhead, J., Jackson, N.L., 1996. Indeterminacy in aeolian sediment transport across beaches. J. Coast Res. 12, 641–653.

Baykal, C., Tarakcıoğlu, G.Ö., Aydın, D., Çınar, G., 2017. Application of XBeach in a beach nourishment and restoration project a case study: alanya-Turkler, Turkey. In: XBeach X (10th Year Anniversary) Conference, pp. 1–3.

Brand, E., Ramaekers, G., Lodder, Q., 2022. Dutch experience with sand nourishments for dynamic coastline conservation – an operational overview. Ocean Coast Manag. 217, 106008 https://doi.org/10.1016/j.ocecoaman.2021.106008.

Bruun, P., 1962. Sea-level rise as a cause of shore erosion. J. Waterw. Harb. Div. 88 (1), 117–132.

Bruun, P., 1954. Coast Erosion and the Development of Beach Profiles, Beach Erosion Board Technical Memorandum. US Beach Erosion Board, US Army Engineer Waterways Experiment Station, Vicksburg.

Cabezas-Rabadán, C., Rodilla, M., Pardo-Pascual, J.E., Herrera-Racionero, P., 2019. Assessing users' expectations and perceptions on different beach types and the need for diverse management frameworks along the Western Mediterranean. Land Use Pol. 81, 219–231. https://doi.org/10.1016/j.landusepol.2018.10.027.

Capobianco, M., De Vriend, H.J., Nicholls, R.J., Stive, M.J.F., 1994. Application of a parametric long term model concept to the Delray beach nourishment program. In: Coastal Dynamics - Proceedings of the International Conference, pp. 391–401.

Chen, W.L., Dodd, N., 2021. A nonlinear perturbation study of a shoreface nourishment on a multiply barred beach. Continent. Shelf Res. 214, 104317 https://doi.org/10.1016/j.csr.2020.104317.

Chen, W.L., Dodd, N., 2019. An idealised study for the evolution of a shoreface nourishment. Continent. Shelf Res. 178, 15–26. https://doi.org/10.1016/j.csr.2019.03.010.

Coelho, C., Larson, M., Hanson, H., 2017. Simulating cross-shore evolution towards equilibrium of different beach nourishment schemes. In: Coastal Dynamics, pp. 1732–1746.

Cooke, B.C., Jones, A.R., Goodwin, I.D., Bishop, M.J., 2012. Nourishment practices on Australian sandy beaches: a review. J. Environ. Manag. 113, 319–327. https://doi.org/10.1016/j.jenvman.2012.09.025.

Davidson, M., 2021. Forecasting coastal evolution on time-scales of days to decades. Coast Eng. 168, 103928 https://doi.org/10.1016/J.COASTALENG.2021.103928.

Davidson-Arnott, R.G.D., 2005. Conceptual model of the effects of sea level rise on sandy coasts. J. Coast Res. 21, 1166–1172. https://doi.org/10.2112/03-0051.1.

Davidson-Arnott, R.G.D., Law, M.N., 1996. Measurement and prediction of long-term sediment supply to coastal foredunes. J. Coast Res. 12, 654–663.

De Schipper, M.A., De Vries, S., Stive, M., De Zeeuw, R., Rutten, J., Ruessink, G., Aarninkhof, S., Van Gelder-Maas, C., 2014. Morphological development of a mega-nourishment; first observations at the sand engine. Coast. Eng. Proc. 1, 73. https://doi.org/10.9753/icce.v34.sediment.73.

De Vriend, H.J., Stive, M.J.F., Nicholls, R.J., Capobianco, M., 1993. Cross-shore spreading of shore nourishment. In: Bruun, P. (Ed.), Proc. Hilton Head Island Coastal Symposium, pp. 175–179.

De Vries, S., Arens, B., Stive, M., Ranasinghe, R., 2011. Dune growth trends and the effect of beach width on annual timescales. In: The Proceedings of the Coastal Sediments 2011. World Scientific Publishing Company, pp. 712–724. https://doi.org/10.1142/9789814355537_0054.

Defeo, O., McLachlan, A., Schoeman, D.S., Schlacher, T.A., Dugan, J., Jones, A., Lastra, M., Scapini, F., 2009. Threats to sandy beach ecosystems: a review. Estuar. Coast Shelf Sci. 81, 1–12. https://doi.org/10.1016/j.ecss.2008.09.022.

Doody, J.P., 2013. Coastal squeeze and managed realignment in southeast England, does it tell us anything about the future? Ocean Coast Manag. 79, 34–41. https://doi.org/10.1016/j.ocecoaman.2012.05.008.

Drijfhout, S., Le Bars, D., 2021. KNMI Klimaatsignaal '21 - Hoe Het Klimaat in Nederland Snel Verandert.

Giardino, A., Werf, J. Van Der, Ormondt, M. Van, 2010. Simulating Coastal Morphodynamics with Delft3D: Case Study Egmond Aan Zee, vol. 80. Deltares Delft Hydraulics.

Haasnoot, M., Kwadijk, J., Van Alphen, J., Le Bars, D., Van Den Hurk, B., Diermanse, F., Van Der Spek, A., Oude Essink, G., Delsman, J., Mens, M., 2020. Adaptation to uncertain sea-level rise; how uncertainty in Antarctic mass-loss impacts the coastal

adaptation strategy of The Netherlands. Environ. Res. Lett. 15, 034007 https://doi.org/10.1088/1748-9326/ab666c.
Hamm, L., Capobianco, M., Dette, H.H., Lechuga, A., Spanhoff, R., Stive, M.J.F., 2002. A summary of European experience with shore nourishment. Coast Eng. 47, 237–264. https://doi.org/10.1016/S0378-3839(02)00127-8.
Hanson, H., Brampton, A., Capobianco, M., Dette, H.H., Hamm, L., Laustrup, C., Lechuga, A., Spanhoff, R., 2002. Beach nourishment projects, practices, and objectives—a European overview. Coast Eng. 47, 81–111. https://doi.org/10.1016/S0378-3839(02)00122-9.
Huisman, B.J.A., Walstra, D.J.R., Radermacher, M., de Schipper, M.A., Ruessink, B.G., 2019. Observations and modelling of shoreface nourishment behaviour. J. Mar. Sci. Eng. 7 https://doi.org/10.3390/jmse7030059.
Huisman, B.J.A., Wang, Z.B., De Ronde, J.G., Stronkhorst, J., Sprengers, C.J., 2013. Coastline modelling for nourishment strategy evaluation. In: 6th SCACR – International Short Course/Conference on Applied Coastal Research.
IPCC AR6 Working Group I, 2021. IPCC, 2021: Climate Change 2021-the Physical Science Basis. https://doi.org/10.3316/informit.315096509383738. Interaction.
IPCC AR6 Working Group II, 2022. IPCC, 2022: Climate Change 2022-impacts, Adaptation and Vulnerability.
Kalligeris, N., Smit, P.B., Ludka, B.C., Guza, R.T., Gallien, T.W., 2020. Calibration and assessment of process-based numerical models for beach profile evolution in southern California. Coast Eng. 158, 103650 https://doi.org/10.1016/j.coastaleng.2020.103650.
Kroon, A., De Schipper, M.A., De Vries, S., Aarninkhof, S., Coelho, B., De Schipper, M., 2022. Subaqueous and Subaerial Beach Changes after Implementation of a Mega Nourishment in Front of a Sea Dike. https://doi.org/10.3390/jmse10081152 researchgate.net.
Lavrentiev, M.M., 2015. Diffusion model identification for long-term coastal profile evolution. In: The Twenty-Fifth International Ocean and Polar Engineering Conference, pp. 1271–1278.
Lippmann, T.C., Holman, R.A., 1989. Quantification of sand bar morphology: a video technique based on wave dissipation. J. Geophys. Res. Oceans 94, 995–1011. https://doi.org/10.1029/JC094iC01p00995.
Luijendijk, A.P., de Schipper, M.A., Ranasinghe, R., 2019. Morphodynamic acceleration techniques for multi-timescale predictions of complex sandy interventions. J. Mar. Sci. Eng. 7 https://doi.org/10.3390/jmse7030078.
Luo, S., Liu, Y., Jin, R., Zhang, J., Wei, W., 2016. A guide to coastal management: benefits and lessons learned of beach nourishment practices in China over the past two decades. Ocean Coast Manag. 134, 207–215. https://doi.org/10.1016/j.ocecoaman.2016.10.011.
Marinho, B., Coelho, C., Larson, M., Hanson, H., 2017. Simulating cross-shore evolution towards equilibrium of different beach nourishment schemes. In: Coastal Dynamics, pp. 1732–1746.
McCarroll, R.J., Masselink, G., Valiente, N.G., Scott, T., Wiggins, M., Kirby, J.A., Davidson, M., 2021. A rules-based shoreface translation and sediment budgeting tool for estimating coastal change: ShoreTrans. Mar. Geol. 435 https://doi.org/10.1016/J.MARGEO.2021.106466.
McLachlan, A., Defeo, O., Jaramillo, E., Short, A.D., 2013. Sandy beach conservation and recreation: guidelines for optimising management strategies for multi-purpose use. Ocean Coast Manag. 71, 256–268. https://doi.org/10.1016/j.ocecoaman.2012.10.005.
Montaño, J., Coco, G., Antolínez, J.A.A., Beuzen, T., Bryan, K.R., Cagigal, L., Castelle, B., Davidson, M.A., Goldstein, E.B., Ibaceta, R., Idier, D., Ludka, B.C., Masoud-Ansari, S., Méndez, F.J., Murray, A.B., Plant, N.G., Ratliff, K.M., Robinet, A., Rueda, A., Sénéchal, N., Simmons, J.A., Splinter, K.D., Stephens, S., Townend, I., Vitousek, S., Vos, K., 2020. Blind testing of shoreline evolution models. Sci. Rep. 10, 1–10. https://doi.org/10.1038/s41598-020-59018-y.
Ranasinghe, R., 2020. On the need for a new generation of coastal change models for the 21st century. Sci. Rep. 10, 1–6. https://doi.org/10.1038/s41598-020-58376-x.
Ranasinghe, R., 2016. Assessing climate change impacts on open sandy coasts: a review. Earth Sci. Rev. https://doi.org/10.1016/j.earscirev.2016.07.011.
Ruggiero, P., Komar, P.D., McDougal, W.G., Beach, R.A., 1997. Extreme water levels, wave runup and coastal erosion. In: Coastal Engineering 1996. American Society of Civil Engineers, New York, NY, pp. 2793–2805. https://doi.org/10.1061/9780784402429.216.
Schooler, N.K., Dugan, J.E., Hubbard, D.M., 2019. No lines in the sand: impacts of intense mechanized maintenance regimes on sandy beach ecosystems span the intertidal zone on urban coasts. Ecol. Indicat. 106, 105457 https://doi.org/10.1016/j.ecolind.2019.105457.
Stive, M.J.F., de Schipper, M.A., Luijendijk, A.P., Aarninkhof, S.G.J., van Gelder-Maas, C., van Thiel de Vries, J.S.M., de Vries, S., Henriquez, M., Marx, S., Ranasinghe, R., 2013. A new alternative to saving our beaches from sea-level rise: the sand engine. J. Coast Res. 290, 1001–1008. https://doi.org/10.2112/JCOASTRES-D-13-00070.1.
Stive, M.J.F., de Vriend, H.J., 1995. Modelling shoreface profile evolution. Mar. Geol. 126, 235–248. https://doi.org/10.1016/0025-3227(95)00080-I.
Stive, M.J.F., Nicholls, R.J., de Vriend, H.J., 1991. Sea-level rise and shore nourishment: a discussion. Coast Eng. 16, 147–163. https://doi.org/10.1016/0378-3839(91)90057-N.
Stronkhorst, J., Huisman, B., Giardino, A., Santinelli, G., Santos, F.D., 2018. Sand nourishment strategies to mitigate coastal erosion and sea level rise at the coasts of Holland (The Netherlands) and Aveiro (Portugal) in the 21st century. Ocean Coast Manag. 156, 266–276. https://doi.org/10.1016/j.ocecoaman.2017.11.017.
Tonnon, P.K., Huisman, B.J.A., Stam, G.N., Rijn, L.C. Van, 2018. Numerical modelling of erosion rates , life span and maintenance volumes of mega nourishments. Coast Eng. 131, 51–69. https://doi.org/10.1016/j.coastaleng.2017.10.001.
Tonnon, P.K., Huisman, B.J.A., Stam, G.N., van Rijn, L.C., 2018. Numerical modelling of erosion rates, life span and maintenance volumes of mega nourishments. Coast Eng. 131, 51–69. https://doi.org/10.1016/j.coastaleng.2017.10.001.
Valdemoro, H.I., Jiménez, J.A., 2006. The influence of shoreline dynamics on the use and exploitation of mediterranean tourist beaches. Coast. Manag. 34, 405–423. https://doi.org/10.1080/08920750600860324.
Valverde, H.R., Trembanis, A.C., Pilkey, O.H., 1999. Summary of beach nourishment episodes on the U.S. East coast barrier islands. J. Coast Res. 15, 1100–1118.
van der Spek, A.J.F., de Kruif, A.C., Spanhoff, R., 2007. Richtlijnen Onderwatersuppleties.
van Duin, M.J.P., Wiersma, N.R., Walstra, D.J.R., van Rijn, L.C., Stive, M.J.F., 2004. Nourishing the shoreface: observations and hindcasting of the Egmond case, The Netherlands. Coast Eng. 51, 813–837. https://doi.org/10.1016/j.coastaleng.2004.07.011.
Van Koningsveld, M., Mulder, J.P.M., 2004. Sustainable coastal policy developments in The Netherlands. A systematic approach revealed. J. Coast Res. 20, 375–385. https://doi.org/10.2112/1551-5036(2004)020[0375:SCPDIT]2.0.CO;2.
Verhagen, H.J., 1996. Analysis of beach nourishment schemes. J. Coast Res. 12, 179–185.
Verhagen, H.J., 1993. Method for artificial beach nourishment. In: Coastal Engineering 1992. American Society of Civil Engineers, New York, NY, pp. 2474–2485. https://doi.org/10.1061/9780872629332.189.
Vries, S. De, Southgate, H.N., Kanning, W., Ranasinghe, R., 2012. Dune behavior and aeolian transport on decadal timescales. Coast Eng. 67, 41–53. https://doi.org/10.1016/j.coastaleng.2012.04.002.
Wijnberg, K.M., Kroon, A., 2002. Barred beaches. Geomorphology 48, 103–120. https://doi.org/10.1016/S0169-555X(02)00177-0.
Wijnberg, K.M., Terwindt, J.H.J., 1995. Extracting decadal morphological behaviour from high-resolution, long-term bathymetric surveys along the Holland coast using eigenfunction analysis. Mar. Geol. 126, 301–330. https://doi.org/10.1016/0025-3227(95)00084-C.
Witteveen&Bos, 2006. Evaluatie onderwatersuppleties Noord- en Zuid-Holland. Eindrapport. Witteveen&Bos rapport Rw1472-2.